

THESIS

EXERCISE TRAINING IMPROVES EXERCISE CAPACITY DESPITE PERSISTENT
MUSCLE MITOCHONDRIAL DYSFUNCTION IN THE *TAZ* SHRNA MOUSE MODEL OF
HUMAN BARTH SYNDROME

Submitted by

Michael Scott Claiborne

Department of Health and Exercise Science

In partial fulfillment of the requirements

For the Degree of Master of Science

Colorado State University

Fort Collins, Colorado

Spring 2013

Master's Committee:

Advisor: Adam J. Chicco

Karyn Hamilton
Benjamin Miller
Michael Tamkun

ABSTRACT

EXERCISE TRAINING IMPROVES EXERCISE CAPACITY DESPITE PERSISTENT MUSCLE MITOCHONDRIAL DYSFUNCTION IN THE *TAZ* SHRNA MOUSE MODEL OF HUMAN BARTH SYNDROME

Barth Syndrome is a mitochondrial disease associated with exercise intolerance and cardioskeletal myopathy resulting from mutations in the tafazzin (*taz*) gene. The present study characterized skeletal muscle mitochondrial function and exercise capacity of a *taz* shRNA mouse model of Barth Syndrome (90% *taz*-deficient), and examined the effect of exercise training on these parameters. Mitochondrial respiratory function was assessed, in mitochondria freshly isolated from hindlimb muscles, using an Oroboros O2K respirometer with pyruvate + malate as substrates, oligomycin as an ATP synthase inhibitor, and carbonyl cyanide 4-(trifluoromethoxy) phenylhydrazone (FCCP) to establish maximal activity. A pre-training GXT revealed profound exercise intolerance, which corresponded to reduced respiratory capacity, citrate synthase (CS) and ETC complex 1 protein content of muscle mitochondria in the *taz* vs. age-matched wild-type (WT) mice. Based on the pre-training GXT, exercise training was conducted at 12-17 m/min, 0% grade for 60 min/d, 5d/wk, for 4 wks. Exercise training elicited a 99% increase in GXT run time in the *taz* mice ($P < 0.01$ vs. pre-training), but failed to increase times to those of sedentary WT mice. Training significantly decreased state 3 respiratory capacity of muscle mitochondria from exercised mice (wild type sedentary (WTS): 4992.59 ± 371.35 , wild type exercised (WTX): 3779.60 ± 561.43 , *taz* sedentary (TazS): 2978.50 ± 383.53 , TazS: 1827.55 ± 525.17 (pmolO₂/(s*mg), $P = 0.02$, Sed. vs. Ex.), and significantly decreased mitochondrial CS activity in *taz* mice (WTS: 4.48 ± 0.51 , WTX: 3.87 ± 0.69 , TazS: 3.21 ± 0.54 ,

taz exercised (TazX): 1.63 ± 0.69 (relative absorbance/gram of protein) (RU/g), $P = 0.01$).

Training also tended to reduce mitochondrial lactate dehydrogenase (LDH) and monocarboxylate transporter 1 (MCT1) activities, MnSOD content, and 4-hydroxnonenal-protein adducts (index of oxidative stress), but tended to increase mitochondrial UCP3 in exercised WT and *taz* mice.

Interestingly, training significantly increased muscle levels of CS (WTS: 1.491 ± 0.112 , WTX: 1.792 ± 0.143 , TazS: 1.325 ± 0.108 , TazX: 1.550 ± 0.143 (RU/g), $P = 0.05$ Sed. v. Ex.), suggesting increased muscle mitochondrial content with training. This study indicates that exercise training improves functional capacity of *taz* deficient mice and induces selective mitochondrial protein remodeling during mitochondrial biogenesis that perhaps mitigates oxidative stress while adapting to increased metabolic demand.

ACKNOWLEDGMENTS

I am grateful to Dr. Adam Chicco for taking a risk on me and letting me work in his lab. His excitement and willingness to pursue any idea made research an adventure. Additionally, Catherine Le was instrumental in the production and completion of this work. Her guidance through the methods was indispensable to productivity and sanity.

My fellow graduate teaching assistants were a constant source of relief and life. Going through graduate school without them would have been a boring and lonely experience. My family was consistently encouraging and supportive, and I especially need to thank my parents for not bringing up my thesis unless I did. Of course I must thank my brother Tom for his support and presence. Without his air and support, this project could not have been completed to the degree that it has been. Semper Fi, Tom. Finally I must thank God for comforting me and strengthening me through all the ups and downs of graduate school.

TABLE OF CONTENTS

ABSTRACT.....	ii
ACKNOWLEDGMENTS	iv
CHAPTER I: Introduction	1
CHAPTER II: Literature Review.....	5
CHAPTER III: Methods and Procedures.....	23
CHAPTER IV: Results	32
Chapter V: Discussion	45
References.....	51
APPENDIX I: Modified Skeletal Muscle Mitochondrial Isolation Procedure.....	62
APPENDIX II: Permeabilized Fibers	65

CHAPTER I

INTRODUCTION

Barth syndrome (BTHS) is an X-linked, recessive mutation of the ubiquitously expressed tafazzin gene [1, 2]. Undiagnosed and untreated, children with BTHS die in early infancy due to cardiomyopathy induced heart failure or neutropenia induced septicemia [1-3]. BTHS is characterized by relapsing episodes of heart failure, neutropenia, growth retardation, muscle weakness, skeletal muscle myopathy, and 3-methylglutaconic aciduria—the biochemical marker of BTHS [1, 2]. These conditions arise from the mitochondrial dysfunction associated with malfunctioning Tafazzin proteins. Tafazzin bends membranes by transacylating phospholipids into a thermodynamically preferential arrangement such that the free energy of the packed lipids is at a minimum. This remodeling aggregates more unsaturated phospholipids at the bends of folded membranes and aligns saturated phospholipids with straight acyl fatty acid chains in the straighter portions [4]. Due to dysfunctional Tafazzin in BTHS, intercrisae spaces do not consistently form or intermembrane spaces fail due to a lack of stable bends, inhibiting the function of BTHS mitochondria. As a result of malformed membranes, BTHS cardiac mitochondria are markedly enlarged with disorganized, circularly layered cristae [5]. Skeletal muscle mitochondria are not as enlarged as cardiac mitochondria, but contain similarly onion-like cristae with dense granules. Additionally, skeletal muscle (SM) mitochondria have impaired respiration and cytochrome *c* levels are abated [2, 5]. However, despite decreased coupling and impaired state-3 respiration, the ability of Tafazzin deficient mitochondria to produce ATP is maintained [6].

To further study BTHS, a short-hairpin RNA (shRNA) inducible Tafazzin knockdown (*taz*) mouse was developed by TaconicArtemis GmbH (Köln, Germany), under contract with the BTHS foundation [7, 8]. After 8 months of age, or in newborns subjected to 3-10 times the standard dose of Doxycycline, *taz* mice develop mitochondrial, cardiac, and SM characteristics mirroring BTHS [7-9]. It has been hypothesized that increased metabolic demand, such as exercise, might cause the mitochondrial, muscular, and cardiac phenotypes to appear earlier in the *taz* mouse [7, 8]. Increased metabolic demands, such as exercise, may also translate into an exacerbated BTHS phenotype in humans. Because exercise training has been proposed as an additional potential therapy for BTHS (<http://www.clinicaltrials.gov/ct2/show/NCT01194141>) [10], studying the response to exercise training in *taz* mice has taken on significant importance.

Rodents and humans adapt to exercise training in a similar fashion: Absolute and relative VO_{2max} , economy, and efficiency improve [11, 12]; body mass decreases, relative to sedentary controls, with a consistent increase in exercised-limb weight [13-16]; exercised limbs shift to more oxidative or slower twitch fiber types [13]; heart mass increases, both absolutely and relative to body weight; cardiac output increases due to increased ventricular chamber volumes, cardiomyocyte hypertrophy, increased chamber weights, and improved contractile function [14]. These adaptations occur across a variety of modalities, durations, and intensities of exercise and whether exercise is forced or voluntary [17-19]. Exercise training has also been demonstrated to improve metabolic parameters and survivability in mice with metabolic and mitochondrial disease as well as aged mice [15, 20, 21]. However, exhaustive training paradigms can impair adaptation, similar to “overtraining” in humans [17, 18, 22-24].

Mammalian skeletal muscle SM adapts to exercise through increases in mitochondrial content, substrate utilization (lipid utilization for oxidative exercise and carbohydrate for more

glycolytic exercise training), and contractile filament alterations (more oxidative and slower twitch fibers with more oxidative training and more fast twitch glycolytic fibers with more glycolytic training). Mitochondrial biogenesis occurs in response to muscle contraction, Ca^{2+} flux, oxidative stress, and increased ATP turnover [23, 25-28]. Mitochondria also respond to exercise stress through the induced production of and import of antioxidants and increasing proton flux via upregulated uncoupling proteins [25, 26, 29-32]. Uncoupling protein 3 (UCP3) is upregulated during fasting and exercise, likely due to increased levels of fatty acid anions, fatty acid peroxides, and n-6 polyunsaturated fatty acid [22, 33-47]; UCP3 mediated H^+ transport requires fatty acids for activation [42, 43]. UCP3^{-/-} mice exposed to exercise and fasting experience significantly greater oxidative damage and their mitochondria are more coupled; although, non-fasting fatty acid oxidation is not impaired [48, 49]. Changes in *taz* coupling with exercise may potentially be due to membrane irregularities or normal adaptations to exercise such as UCP3 upregulation.

Within *taz* mouse SM, increases in lactate metabolism in response to exercise may be reflective of a shift toward increased reliance on glycolytic metabolism during exercise as a method of adaptation. *Taz* mice may be abnormally inclined toward anaerobic pathways due to their impaired mitochondrial function. In the SM of WT mice, total LDH activity either does not change or decreases with chronic exercise [50-53]. In the heart, trends for total LDH activity are the opposite—no change or an increase [51, 53]. Decreases in total LDH activity are fiber type specific, with greater decreases in oxidative fiber types than in glycolytic fiber types [50-52]. Along with these shifts, LDH isoforms change from muscle-LDH to more heart-LDH, favoring the conversion of lactate to pyruvate and an increased lactate utilization as a fuel source [51, 53]. Lactate transport and clearance also increase with exercise [54, 55]. Lactate transport is

facilitated by increased MCT1 and -4. MCT1 protein content increases linearly with exercise duration and intensity until exercise becomes exhaustive, at which point MCT1 protein levels decrease [24, 56-65]. MCT1 levels may be considered a necessary covariate of changes in lactate metabolism, with MCT1 levels increasing with increased reliance on lactate and decreasing with less reliance on lactate.

The proposed use of exercise as a therapy for BTHS has prompted this study of the effects of 4 weeks of progressive treadmill running on the performance and mitochondrial phenotype of *taz* SM. Such phenotypes may not be apparent in mice that are limited to sedentary cage activity, which necessitates the examination of increased metabolic demand on the *taz* mouse.

CHAPTER II

LITERATURE REVIEW

Barth Syndrome and Tafazzin Deficiency

Barth syndrome (BTBS) is an X-linked, recessive mutation of the ubiquitously expressed tafazzin gene [1, 2]. Undiagnosed and untreated, children with BTBS die in early infancy due to cardiomyopathy induced heart failure or neutropenia induced septicemia [1-3]. Previously, only male BTBS had been described; however, recently, a female case was described with relapsing episodes of heart failure, neutropenia, growth retardation, and muscle weakness and skeletal muscle myopathy, which, along with 3-methylglutaconic aciduria—the biochemical marker of BTBS—are the primary symptoms of BTBS [1, 2, 66].

The examination of cardiac and SM biopsies of BTBS patients has revealed an array of cellular abnormalities. In type I SM fibers, intramuscular fat droplets occupy an increased area [2]. BTBS tissues also have decreased unsaturated fatty acid levels with elevated saturated fatty acid concentrations [5]. Most remarkable in BTBS tissues are mitochondrial abnormalities. Cardiac mitochondria are markedly enlarged with disorganized, circularly layered cristae [5]. Skeletal muscle mitochondria, while not as conspicuously enlarged as cardiac mitochondria, contain similarly onion-like cristae with dense granules. Additionally, SM mitochondria have impaired respiration and cytochrome *c* levels are abated [2, 5]. These observations initially led to BTBS being thought of as a condition of mitochondrial dysfunction resulting from the loss of function of the tafazzin protein.

Tafazzin, Cardiolipin, and Membrane Formation

Tafazzin deficiency associated with BTHS was first thought to be related to improper Cardiolipin (CL) remodeling. Cardiolipin is a tetra-acyl phospholipid localized primarily within the inner mitochondrial membrane and is essential to the structure and function of several mitochondrial proteins, including complexes I, III, IV, and V [1, 67, 68]. In BTHS, the deacylation-reacylation cycle that eventually converts CL into tetralinoleoyl CL (L₄CL)—the most abundant CL species in the mammalian heart—was thought to be impaired by the mutation of Tafazzin due to the decreased incorporation of linoleic acid (18:2) [1, 67, 69]; indeed, biopsies of Barth patients reveal normal concentrations of CL but low L₄CL [70]. Irregular CL speciation may disrupt mitochondrial processes by impairing protein function and disrupting membrane formation and folding. However, despite abnormal CL formation and decreased coupling and impaired state-3 respiration, the ability of Tafazzin deficient mitochondrial to produce ATP is maintained, suggesting that the significance of Tafazzin is not limited to CL formation or speciation as it pertains to mitochondrial membrane integrity [6]. Additionally, despite homologous human *Tafazzin* gene incorporation, transgenic yeast and *drosophila* strains fail to demonstrate any acyl-specificity of Tafazzin [71-73]. A lack of acyl-specificity suggests that improper CL speciation does not necessarily lead to mitochondrial dysfunction.

Recent work by Schlame *et al.* (2012) further clarified the function of Tafazzin. Their work demonstrated that Tafazzin's action is based on thermodynamic remodeling: Tafazzin transacylates membrane acyl groups until the free energy of the packed lipids is at a minimum. Tafazzin bends membranes by transacylating phospholipids (PL), regardless of acyl group, into a thermodynamically preferential arrangement. Unsaturated PL—such as L₄CL—will be aggregated at cristae bends because they occupy more space, and more densely aligning

saturated PL will be aligned in linear portions of the cristae. In BTHS, intercristae spaces do not form, or the spaces fail due to a lack of stable bends, inhibiting the function of BTHS mitochondria [4].

However, Tafazzin's membrane folding action does not appear to be limited to mitochondrial membranes, and it may extend to all highly folded, lipid membranes. In *Tafazzin* knockdown mice, the brush boarder of the jejunum, as assessed by high-level light microscopy, appears to be significantly disrupted compared to the brush boarder of wild type mice (unpublished observations).

The Taz mouse: a mammalian model of human Barth Syndrome

TaconicArtemis GmbH (Köln, Germany), under contract with the BTHS foundation, developed an shRNA-mediated knockdown murine model of human BTHS. Doxycycline (dox) feeding induces an 88 to >96% knockdown of *taz* mRNA levels in SM, liver, and brain [7, 8]. If mice are taken off of dox at 4 weeks of age, there is a partial recovery of 48-64% of *taz* mRNA in heart, SM, and liver 4 weeks and 2 months later [7].

After 2 months of dox feeding, mtDNA is elevated 30% in SM and 4-fold in the heart; changes in mtDNA are not observed in other tissues [7]. This increase in mtDNA may imply enhanced mitochondrial biogenesis. Despite changes in mtDNA, Acehan *et al.* (2011) did not observe any mitochondrial changes after 2 months [7]. However, Soustek *et al.* (2011) observed swirled mitochondria with disrupted cristae among normal mitochondria at 2 months [8]. Surprisingly, Acehan used a greater dox dose (625 mg/kg of chow) than Soustek (200 mg/kg of chow) [7, 8]. Despite changes in mitochondria, neither study observed functional changes in cardiac or SM function [7, 8]. By contrast, newborn mice subjected to 3-10 times the dose of dox

used by Soustek or Acehan, demonstrated cardiac noncompaction, hypertrabeculation, myocardial thinning, and defective ventricular septation. Within SM, the parallel alignment of mitochondria and sarcomeres was irregular. Additionally, mitochondria were vacuolated, reduced in area, and had diminished cristae density [9]. The time course and dose of dox appear to be able to variably affect the degree of the *taz* knockdown.

After 8 months of dox exposure, *taz* mice develop mitochondrial, cardiac, and SM characteristics tightly mimicking BTHS. Cardiolipin species of 72:8 and 72:7 CL were lowered to 2 and 3%, respectively, of CL species from the 19 and 15% observed in WT mice [7]. Within the mitochondria, the cristae were disorganized or collapsed. The mitochondria appeared larger with a stacked or onion-like structure, although net mitochondrial area was not different than WT mice. In striated tissues, the parallel arrangement of mitochondria and sarcomeres was disrupted. *Taz* hearts exhibited left ventricular dilation, left ventricular mass reduction, and depressed fractional shortening and ejection fraction [7, 8]. Within the soleus, *Taz* knockdown resulted in reduced isometric-contraction strength at 100hz and 160hz of electrical stimulation [8]. Additionally, at 8 months *taz* mice weighted 17% less than WT dox-treated littermates [7]. Despite these respiratory and functional deficiencies, no locomotor differences were observed between *taz* and WT mice [8].

Both the Acehan and Soustek groups hypothesized that increased metabolic demand, such as exercise, might cause the mitochondrial, muscular, and cardiac phenotypes to appear earlier the *taz* mouse—to the mouse's detriment, of course [7, 8]. Because exercise training has been proposed as an additional potential therapy for BTHS (<http://www.clinicaltrials.gov/ct2/show/NCT01194141>) [10], studying the response to exercise training in *taz* mice has taken on significant importance.

Murine Response to Exercise Training

Because of the benefits and physiological effects of exercise, pursuing exercise as a potential therapy for BTHS may make sense as a means of improving general living functionality. However, because exercise can impose a significant physiological stress and metabolic demand, relatively higher degrees of exercise intensity may not be appropriate for those whose bodies are already under significant stress, such as BTHS patients. The purpose of the present study is to examine the effects of exercise on *taz* mouse exercise performance and SM mitochondrial function. Exercise performance is used as a basic measure of overall health; better exercise performance should indicate improved everyday functionality. Mitochondrial function is examined because of the initial characterization of BTHS as a mitochondrial dysfunction, and because mitochondria are a primary site of exercise adaptation. Here the effects of exercise on mitochondrial biogenesis, leak, UCP3 proteins, and MCT1 proteins and lactate metabolism within mouse and rat models will be reviewed.

Typical Response to Exercise

Rats and mice exposed to exercise programs consistently demonstrate increased cardiac output due to increased ventricular chamber volumes, cardiomyocyte hypertrophy, increased chamber weights, and improved contractile function [14]. Heart mass increases are both absolute and relative to body weight [14]. Absolute and relative VO_{2max} , economy, and efficiency also improve in rodents subjected to exercise [11, 12]. Typically the exercise groups lose body mass relative to sedentary controls with a consistent increase in exercised-limb weight, but this is not always the case [13-16]. Exercised limbs also experience a shift to more oxidative or slower

twitch fiber types [13]. These changes have been observed in rat and mouse models under forced treadmill running, voluntary wheel running, and forced swimming training models [17-19].

There is some variation in the degree and type of cardiac response elicited from different intensities of exercise. Rats exposed to a high stress exercise program can experience significant increases in left and right ventricular mass, and impaired contractile function after 6 weeks but not 10 [17, 22]. Rats under a high-stress protocol also demonstrate an increase in capillary-to-mitochondrial wall distance with a concomitant decrease in capillary density [17]. An extended period (six weeks) of high intensity (16% grade) exercise also decreases state 3 respiration [22]. Opposite trends are observed in rats run under milder training paradigms. Rats exposed to milder programs had a significant increase in right ventricular mass or overall cardiac mass without any impairment of contractile function [18, 22]. Under the milder exercise conditions reported by Anversa *et al.* (1982 & 1983) capillary density increased and the distance from capillary to mitochondria decreased, but there were no significant changes in mitochondrial density [17, 18, 22]. The above adaptations are all associated with oxygen delivery, which is essential for mitochondrial respiration. Dysfunctional mitochondria may also impair higher order adaptations to exercise because mitochondria are not able to use the already available oxygen, however that should not necessarily eliminate the signaling to increase oxygen delivery adaptations. How *taz* mice will adapt to exercise cannot be definitively asserted based on previous experiments on healthy animals.

Exercise in Diseased Mice

Because the adaptations of healthy mice and rats may not translate to diseased mouse models, it is worthwhile to examine some mice with varying degrees of different mitochondrial

dysfunction. Mice with cytochrome-c (COX) oxidase deficiency develop mitochondrial myopathy and have a decreased lifespan. Exercise was proposed to potentially exacerbate their condition because they exist in a metabolically stressed state. However, exercising these mice nearly doubled and tripled the life expectancy of the male and female mice, respectively. COX10 KO mice experienced expected adaptations to exercise in that training increased the proportion of oxidative fiber types and increased PGC-1 α , leading to increased mitochondrial biogenesis, which was also observed via the enhanced OXPHOS capacity of the mice [20]. Physical Activity also attenuates the loss of skeletal muscle mass in old mice [21]. And, in hyperglycemic rats, exercise reversed elevated hyperglycemia-induced Cyclophilin D (mitochondrial permeability regulator) levels, and increased adenine nucleotide translocase (ANT) transcription factor A (an ADP/ATP exchanger and mechanism for controlling mitochondrial leak). Ca²⁺ uptake increased and Ca²⁺ release decreased, indicating tighter Ca²⁺ homeostasis, the loss of which can exacerbate apoptotic signaling [15]. Overall, these changes represent beneficial adaptations to exercise, particularly beneficial adaptations to exercise that benefit mitochondrial function, which may explain any benefits of exercise within the *taz* mouse and hint that exercise will likely benefit the *taz* mouse.

Mitochondrial Expansion

Mitochondrial mass has consistently been shown to expand with exercise training; the mechanisms, timeframe, the qualitative degree, and the functionality of mitochondrial expansion resulting from training continue to be further defined and elucidated under a variety of metabolically challenged states. Contractile and metabolic activity accelerate ATP turnover, and exercise exacerbates the difference between cellular ATP demands and mitochondrial ATP

production. Exercise mediated contractile activity also affects mitochondrial Ca^{2+} flux between extracellular spaces, the cytosol, and mitochondria [25]. The increases in O_2 flux associated with accelerated ADP phosphorylation generate reactive oxygen species (ROS), which also act as potent mediators of mitochondrial biogenesis [23, 26-30].

Hood (2001) has reviewed the literature related to contractile activity and mitochondrial expansion [25]. In brief, perturbations in Ca^{2+} and increased ATP turnover activate a variety of kinases, which phosphorylate several transcription factors. After contractile activity shifts in ATP and Ca^{2+} homeostasis increase mRNA for cytochrome *c*, mitochondrial transcription factor A (Tfam), *c-jun*, and nuclear respiratory factor-1. These newly transcribed proteins will have a half-life of approximately 1 week, and mitochondrial phospholipids will last about 4 days. These changes in mRNA have been used to indicate the degree and potential duration of mitochondrial biogenesis as a result of contractile activity. Similar adaptations may be expected to take place in the *taz* mice. In the case of BTHS patients, in humans, it is generally well accepted that after 6 weeks of training, humans can expand their mitochondrial content by 50 to 100% [25], this hopefully provides some measure of the translatability of exercise in non-BTHS humans to BTHS patients particularly if adaptations are observed in the *taz* mice.

In animal models, significant increases in mitochondrial protein content have consistently been observed but with great variation in the degree and time course. Originally, an expansion of mitochondrial protein content was observed by Holloszy in 1967 after strenuously training rats for 12 weeks; cytochrome *c* increased two-fold while total mitochondrial protein content increased 60% [30]. Mole *et al.* made similar observations in 1971, also finding a 60% increase in mitochondrial protein content with exercise [74]. Increases in training time and intensities both produce positive, linear relationships in mitochondrial expansion and several later studies

confirmed mitochondrial expansion in a variety of fiber types and in old and young animals [12, 15, 16, 21, 75-77]

The timeframe during which mitochondrial adaptations take place appears to be rapid; although, longer periods have been observed to be necessary for mitochondrial expansion. Tfam has been shown to increase after 5 days of training and CS to increase 29% and 39% after 5 and 10 days of training, respectively [78, 79]. However, similar time courses in mitochondrial adaptation to exercise have not been observed in all rodent exercise models: after progressively training guinea pigs for 9 and 18 weeks, significant increases in mitochondrial protein content and O₂ consumption were only observed after 18 weeks [80]. However, mitochondrial adaptation appears to be rapid in rat and murine models [25].

Adaptation to Oxidative Stress

Mitochondrial expansion serves roles beyond increasing a cell's ATP production capacity. Mitochondrial expansion, in theory, should lower mitochondrial membrane potentials ($\Delta\Psi$), thereby moderating free radical and ROS production, by distributing the proton gradient across a wider area. There will be more mitochondria producing ATP at a lower rate while being exposed to lesser $\Delta\Psi$ rather than having a small volume of mitochondria working maximally while being exposed to greater and more ROS producing $\Delta\Psi$.

Exercise induces mitochondrial adaptation to oxidative stress because exercise is itself an acute oxidative stress--one which should mitigate net oxidative stress through adaptation [23, 26, 28, 29]. Exercising rats to exhaustion produces a two- to three-fold increase in free radicals concentration, diminished mitochondrial respiratory control, increased lipid peroxidation products, diminished sarcoplasmic and endoplasmic reticulum integrity, and decreased

mitochondrial respiratory control [23]. In response to exercise induced oxidative stress mitochondrial volume expands, protein levels changes, H₂O₂ production is decreased and NRF-1, superoxide dismutase-2 levels, manganese superoxide dismutase (MnSOD), and Glutathione peroxidase-4 levels rise [23, 26, 29, 30, 78, 81]. These compensatory mechanisms either moderate free radical production or mitigate ROS after the fact.

Beyond expanding the mitochondrial reticulum and antioxidant production, ROS mitigation lowered $\Delta\Psi$ can be achieved by making mitochondrial membranes more permeable to protons. Within the context of exercise adaptation, increasing proton leak contradicts the increased ATP demand that exercise places on mitochondria, but exercise adaptation is a balancing act between ATP demand and accelerated ROS production.

Mitochondrial Leak

Mitochondrial proton leak can account for as much as 50% of oxygen consumption in isolated muscle fibers and 20-70% in other cell types [82-85]. Leak may account for 25% of standard metabolic rate in rats [83]. Although proton leak diminishes mitochondrial efficiency in terms of ATP produced per oxygen unit utilized, proton leak is thought to facilitate heat production, promote cellular steady-state regulation, maintain carbon flux, and mitigate ROS production; these roles of leak have been further reviewed by Divakaruni and Brand [41]. Due to the oxidative and energetic stresses of exercise and its locus within mitochondria, leak and the means of regulating leak in response to exercise are worth examining.

Greater than 50% of basal leak has been attributed to ANT, independent of the ADP-ATP exchanging role of ANT [86]. Membrane acyl composition also affects leak as well. There is a positive correlation between unsaturated mitochondrial membranes and leak [87-89]; although,

membrane permeability accounts for only 5% of proton leak [90]. At rest, state 4 respiration, which is frequently used as a surrogate measure for leak, is negligibly affected by low levels of oxidative phosphorylation, ANT-mediated ATP/ADP exchange, and uncoupling protein mediated respiration [31, 91]. However, with exercise, state 4 respiration can be increased 50%, an increase which is 50-57% attributable to uncoupling protein 3 (UCP3) [31, 32].

Ageing also increases leak. Old mice (30 months) exhibit a 50% reduction in mitochondrial P/O ratio (ATP phosphorylation to oxygen consumed) relative to younger mice (7 months); oxygen consumption remains the same from young to old mice, but ATP production is down 30%, indicating greater uncoupling [92].

Uncoupling Protein 3

Uncoupling proteins allow for controlled proton leak under specific metabolic conditions. Uncoupling protein-1 (UCP1), the archetype uncoupling protein, has been widely observed to facilitate thermoregulation and thermo-adaptation through non-shivering thermogenesis by uncoupling oxidative phosphorylation in the mitochondria of brown adipose tissue (BAT) [41, 93, 94]. UCP3 is thought to function in a similar fashion as UCP1 and other uncoupling proteins, which are all tightly transcriptionally regulated, activated by fatty acids, and inhibited by purine nucleotides [41, 42, 85, 95-99]. The different UCPs are also not uniformly distributed across tissues, but UCP3 is highly expressed in skeletal muscle and, to a much lesser extent, in cardiac muscle and BAT [100, 101]. Despite its presence in BAT, UCP3 does not appear to be related to thermoregulation [33, 35, 91]. Rather, the role of UCP3, particularly in SM, may be related to relieving oxidative stress by increasing proton conductance, an idea first proposed by Papa and Skulachev in 1997 [102].

UCP3 alone does not affect basal proton conductance and has only been demonstrated to do so in UCP3 overexpressing mice with supraphysiological levels of UCP3 [91, 103]. Rather than uncoupling basal proton conductance, UCP3 appears to catalyze uncoupling in the presence of activators, which are associated with oxidative stress and fat metabolism (fatty acid anions; fatty acid peroxides; 4-Hydroxynonenal (HNE); and C18 and C20 n-6 polyunsaturated fatty acids) [41-46]. UCP3-mediated H^+ transport requires fatty acids for activation, and fatty acid activation largely explains UCP3's presence in BAT and why UCP3 and UCP3-mediated proton conductance have been consistently demonstrated to increase under fasting and exercised conditions [22, 33-40, 42, 43]. The proton conductance associated with exercise may be particularly apparent because exercise represents both an acute oxidative stress and a period of elevated lipid oxidation.

Despite increased UCP3 with exercise and fasting, the degree and function of the increases in UCP3 associated with exercise and fasting have been variable. Brief starvation, extended calorie restriction, and high-fat refeeding have demonstrated increases in UCP3 from 1.5-fold to 4-fold [33, 36, 103]. Similar increases in UCP3 with fasting have been reported in humans as well [104]. Furthermore, during high-fat refeeding after fasting, UCP1, -2, and -3 decrease in SM and increase in adipose tissue [35]. Even though UCP3 is upregulated under fat oxidizing conditions, it is not necessary for fatty acid transport or fatty acid oxidation (FAO), but UCP3 does appear to support enhanced fasting-induced FAO by exporting fatty acid anions, preserving CoAsh, and preventing lipotoxicity, overall, moderating FAO induced ROS production [45, 46, 49, 105]. These roles are further supported by observations of increased oxidative stress in UCP^{-/-} mice under fasted conditions [49]. UCP^{-/-} mice are unable to mitigate the ROS from FAO to the same degree as their WT counterparts, and as a result are subject to

greater oxidative damage. However, increased UCP3 has also failed to demonstrate changes in proton leak, $\Delta\Psi$, and state 4 respiration, and even with greater $\Delta\Psi$, UCP3^{-/-} mice have been shown to have indistinguishable state 4 from WT mice. These discrepancies have been attributed to UCP3 increasing concomitantly with mitochondrial biogenesis, so oxidative stress may still be mitigated, but UCP3 may not be necessary for the mitigations [36, 106]

Elevated FAO during exercise appears to be the predominant factor driving upregulation of UCP3 protein and mRNA content with exercise. Acute exercise consistently demonstrates the most profound and maintained elevations in UCP3 protein and mRNA. Exercise bouts as short as 30 min can significantly increase UCP3 mRNA and bouts of greater than 150 minutes report increases in UCP3 mRNA ranging from a 1.22- to 15- to 200-fold, with greater increases always occurring in fast-twitch/glycolytic fibers and substantially lower or negligible increases in oxidative fibers [91, 107, 108]; increases in mRNA subside after 2 hours and return to baseline between 4 and 22 hours after exercise [40, 108]. UCP3 protein expression, by contrast, only increases 7- to 8-fold with acute exercise [31, 47]. One report has demonstrated an 84% increase in UCP3 up to 10 days after an acute, low-intensity, long-duration training [37]. These elevations in mRNA and protein have been replicated, to a lesser extent, by incubating extensor digitorum longus muscles with 5'-amino-4-imidazolecarboxamide ribonucleoside, which stimulates AMPK activity, mimicking a switch to fatty acids during a calorie restricted state [47]. Effects similar to those just mentioned can be observed with exercise. Throughout the earlier portions of an exercise bout, ROS production rises steadily and increases in UCP3 expression coincide with a drop in respiratory control ratio (RCR)/coupling, potentially moderating ROS production [31]. Additionally, oleic acid has been shown to significantly increase state 4 respiration in trained mitochondria while increasing UCP3 protein, this increase in UCP3 accounts for 50-57% of the

fatty acid-induced uncoupling with exercise [32]. UCP3^{-/-} mice do not exhibit the same change in uncoupling, rather UCP3^{-/-} mice have more coupled mitochondria, produce more ROS, and experience greater oxidative stress after exercise. Despite the oxidative stress imposed on UCP3^{-/-} mice, overexpressors are not protected beyond WT mice [48, 109, 110]. Based on these data, increases in UCP3 content with acute exercise and concomitant uncoupling appear to be attributable to exercise-induced FAO, and UCP3 protein appears to be necessary for protection from elevated FAO-induced oxidative stress.

When exercise training shifts toward a chronic and/or low-intensity paradigm, UCP3 upregulation is lower than with a single bout of acute exercise. Increases in protein expression are limited to 1.5- to 2.3-fold increases [32, 38]; sometimes no increase in UCP3 protein is detectable [34, 107]. These same increases in UCP3 are also tightly paired with increases in markers of elevated mitochondrial content (COX1, cytochrome *c*, citrate synthase (CS)), indicating that long-term increases in UCP3 are likely only an indicator of increased mitochondrial content [32, 37]. Indeed, in humans, utilizing both acute and endurance training, decreases in UCP3 protein have been found--when UCP3 protein is expressed per unit of CS--with the lowest UCP3 levels being found in oxidative fibers. Absolute increases in UCP are typically only observed at the same time that markers for mitochondrial biogenesis are increased [111-113]. From these data it seems likely that as SM increases its oxidative capacity, its need for UCP3 as a protective mechanism declines, and UCP3 is downregulated as a result. This idea is consistent with the low increases in UCP3 observed in red/oxidative fibers in mice and the decline in UCP3 in humans; it is also consistent with the observed drop off of increased UCP3 that parallels the conversion of glycolytic to oxidative fiber type in mice [38]. During exercise,

UCP3 functions to acutely moderate the oxidative stress resulting from increased FAO, and it's role is cut back as SM increases its capacity to oxidize fatty acids during exercise.

MCT1 Response to Exercise

Monocarboxylate transporter-1 and -4 can transport pyruvate, acetate, propionate, butyrate (monocarboxylates), and keto acids derived from transamination [56]. Due to the increased metabolic demands of exercise, the multiplication of substrate transporters such as MCT1 with exercise is a necessary adaptation. MCT1 is predominantly found in oxidative fibers of skeletal muscle (MCT4 is not fiber specific) [56, 63, 114, 115]. The specific locations of MCT1 within SM have been contested. MCT1 has definitively been shown to be present on the sarcolemmal plasma membranes, although to varying degrees, but its presence on and within SM mitochondria is currently uncertain [115-117]. In proximity to mitochondrial populations, MCT1 and -4 appear to be associated with subsarcolemmal mitochondria, but not intermyofibrillar, and whether MCT1 is actually embedded within mitochondrial membranes has been questioned [116-118]. The specific location of MCT1 has direct implications on the location and capacity of SM and mitochondria to metabolize lactate.

MCT1 has consistently been positively associated with lactate release and uptake during exercise [56, 62-64, 115]. In humans, MCT1 content is inversely related to fatigue index [119]. This observation pairs well with the understanding that MCT1 supports the oxidation lactate [63]. MCT transport of lactate appears to be a function of lactate gradients and pH, with greater external lactate concentrations and lower pH speeding transport [55, 56, 120]. However, MCT1 has a ~4.7-fold greater affinity for pyruvate over lactate [121]. In the presence of both pyruvate and lactate, pyruvate will be preferentially transported and lactate left not metabolized. MCT1

protein quantity is generally increased with acute or chronic training and present for 2-6 days post exercise [56-64]; however, exercise intensity does need to overload or pass a threshold before MCT1 protein is upregulated [57]. MCT1 protein increases the most in red or oxidative fiber types [61-63, 114, 115]. But, MCT1 protein increases are only positively correlated with training intensity to a point. Once training becomes “exhaustive,” MCT1 protein may be downregulated and transport capacity impaired [24, 57, 65]. MCT1 can potentially be used as a correlating measure of lactate utilization and as a measure of training efficacy because of its role in lactate transport as well as its function as a substrate transporter.

LDH Activity and Response to Exercise

Despite increases in MCT1 protein with exercise, in SM, total lactate dehydrogenase (LDH) activity either does not change or decreases with exercise [50-53]. In the heart, trends for total LDH activity are the opposite—no change or an increase [51, 53]. Decreases in LDH activity are fiber type specific, with greater decreases in oxidative fiber types than in glycolytic fiber types [50-52]. Along with these shifts, LDH isoforms change from muscle-LDH to more heart-LDH, favoring the conversion of lactate to pyruvate [51, 53]. In light of these activity patterns and isoform changes, lactate appearance is lower and clearance greater after exercise training [54, 55]. In SM there may appear to be no change in LDH activity, but lactate oxidation will likely be increased due to the shift in isoform. Lactate appearance is another factor to consider for future studies as well.

Not only is lactate metabolism worth examining because of a potential shift toward glycolytic metabolism due to impaired mitochondrial respiratory capacity, which would leave open the questions about lactate oxidation post-production. Furthermore, within BTHS the

location of LDH within SM may alter the activity of LDH due to the disruption of mitochondrial membranes in BTHS and *taz* mice. The location and abundance of LDH within SM and SM mitochondria remains controversial [122-125]. Early studies found similar levels of LDH within the mitochondria and the cytosol [126]; however, later studies were unable to demonstrate significant LDH activities above levels that would have been greater than contamination [127]. Given that cytosolic LDH closely adheres to the outer mitochondrial membrane and that even the earlier studies found mitochondrial LDH primarily within the intermembrane space, contamination seems likely [126, 127]. More recent studies have failed to detect LDH activity in isolated mitochondria; some have been unable to detect lactate respiration after the addition of LDH to isolated mitochondria and have only achieved respiration after the addition of NAD⁺ despite normal pyruvate respiration [57, 118, 128, 129]. However, Brooks *et al.* (1999) found robust LDH activity in isolated mitochondria: similar state 3 and 4 respiration, RCR, and P/O ratios between pyruvate and lactate [130].

Additionally, the location of MCT1 has furthered the controversy about the function of LDH within mitochondria. Because MCT1 predominates at the sarcolemmal surface but does not appear to be significantly present in IMF mitochondrial populations, lactate may not be used in the IMF mitochondria because it would not be transported in [115-118]. Furthermore, the reported preference of MCT1 for pyruvate over lactate would not support an intracellular lactate shuttle [121].

Gladden *et al.* (2007) has attempted to synthesize the divergent results by suggesting that, while LDH may not be present within the mitochondrial matrix, MCT1 and LDH may support an intracellular lactate shuttle on the outer mitochondrial membrane and on the outside of the inner mitochondrial membrane [124]. The colocalization of substrates and transporters in close

proximity to the mitochondrial membranes would not only support an intracellular lactate shuttle, but it could account for contamination or loss during isolation.

Despite the controversy around LDH, it remains an important standard of exercise adaptation even though exercise may not necessarily modify mitochondrial lactate metabolism. The difficulty of precisely isolating mitochondria also suggests that it may be more prudent to examine whole muscle LDH activity when assessing *taz* adaptation to exercise.

Purpose

The purpose of this study is to establish the extent of skeletal muscle mitochondrial respiratory dysfunction and exercise intolerance in the *taz* mouse relative to WT counterparts, and determine if increasing metabolic demands via chronic exercise training will rescue or exacerbate the *taz* phenotype. It is hypothesized that exercise will improve exercise capacity in the *Taz* shRNA mice, by increasing skeletal muscle-LDH activity with a concomitant increase in MCT1, elevated UCP3, increased mitochondrial biogenesis, and a recovery of diminished mitochondrial respiration. Little is known about the effect of BTHS on the function of skeletal muscle, and in light of the proposed exercise therapy for BTHS patients, knowledge of its impact may inform therapeutic application.

CHAPTER III

METHODS AND PROCEDURES

All procedures in this investigation were approved by the Colorado State University Care and Use Committee and conform to the *Guide for the Care and Use of Laboratory Animals* published by the US National Institutes of Health (NIH Publication No. 85-23, revised 1996).

Graded exercise testing, progressive treadmill training, and handling.

Forty-eight female WT and *taz* mice (TaconicArtemis GmbH; K^oln, Germany) (C57BL/6J background) were housed in a climate controlled, university, animal care facility and maintained under a 12:12-h light-dark cycle; all mice were housed in the noise conditions of the treadmill and air compressor during training sessions. Handling was partially equilibrated by housing trained and sedentary animals in the same cages. Animals were trained on a 10-lane motorized treadmill specially designed for use in rats. Animals were acclimated to the treadmill across 3 days by being placed on the treadmill at 0 m/min for 5 minutes on day 1, 0 m/min for five minutes and 5 m/min for 1 minute on day 2, and 0 m/min for 5 minutes and 5 m/min for 2 minutes on day 3. Animals were also exposed to compressed air blasts at this time. An initial 0% grade graded exercise test (GXT) was performed to establish an effective GXT protocol. Mice were started at 5 m/min and the belt speed was increased every 2.5 minutes at 2.5 m/min increments. Mice ran to failure, which was established as the delivery of 10 motivational bursts of compressed air within 30s. From the results of the 0% grade GXT, a 20% grade GXT protocol was designed [131-135]. On a 20% grade, mice ran for 2 min at 7 m/min, 1.5 min at 10 m/min, 1.5 min at 12 m/min, 2 min at 15 m/min, 7 min at 20 m/min, 7 min at 22 m/min, and finally at 25

m/min for 9 minutes until the 30 min cutoff. This cutoff produced a ceiling for the GXT for most of the WT mice. This GXT protocol resulted in the exhaustion of all *taz* mice and 5 of the 14 WT mice. After training, the 20% grade GXT was performed again on all mice 48 or 72 hours before takedown to reduce appearance of acute exercise adaptation. Sedentary mice were reintroduced to the treadmill the day before the post-test at 5 min of 0 m/min and 5 min of 7 m/min.

An exhaustive pace of 20 m/min was established for the *taz* mice based on the first 20% grade GXT and was not achieved during training to establish a low-intensity paradigm. After the initial 20% GXT, mice were randomly assigned to training or sedentary groups by an Excel random number generator. After group assignments, t-tests were performed to establish that the pre-test times for the trained groups were not significantly different from the respective genotype's sedentary group's pre-test time. Animals were trained 5 days/week in the last hour of their natural active (dark) cycle (6-7 am).

Training was progressively staged for 4.5 weeks (table 1). The first takedown group of mice began training one day before the others; they were subject to two days of the first stage of training.

Table 1. A complete table of the schedule and all of the training intervals utilized during the training protocol. All training days consisted of a 10 min. warm-up, a long moderate-pace

	Stage 1	Stage 2	Stage 3				Stage 4	Stage 5			
	1-2 days	1 day	1 day	1 day	1 day	4 days	3 days	2 days	7-9 days		
Pret-test GXT	-5 min, 7m/min	-5 min, 7m/min	-5 min, 7m/min	-5 min, 7m/min	-5 min, 7m/min	-5 min, 7m/min	-5 min, 7m/min	-5 min, 7m/min	-5 min, 7m/min	-5 min, 7m/min	Post-test GXT
	-25 min, 12m/min	-20 min, 12m/min	-5 min, 12 m/min								
	-5 min, 7m/min	-5 min, 15m/min	-10 min, 12 m/min	-10 min, 12 m/min	-10 min, 12 m/min	-45 min, 15 m/min	-35 min, 15 m/min	-15 min, 15 m/min	-15 min, 15 m/min	-15 min, 15 m/min	
		-5min, 12m/min	-10 min, 15 m/min	-15 min, 15 m/min	-30 min, 15 m/min	-3 min, 12 m/min	-5 min, 17 m/min	-5 min, 17 m/min	-5 min, 17 m/min	-5 min, 17 m/min	
		-2 min, 7m/min	-10 min, 12 m/min	-5 min, 12 m/min	-5 min, 12 m/min	-2 min, 7m/min	-5 min, 15 m/min	-5 min, 15 m/min	-5 min, 15 m/min	-5 min, 15 m/min	
			-3 min, 12 m/min	-3 min, 12 m/min	-3 min, 12 m/min		-3 min, 12 m/min	-5 min, 17 m/min	-5 min, 17 m/min	-5 min, 17 m/min	
			-2 min, 7m/min	-2 min, 7m/min	-2 min, 7m/min		-2 min, 7m/min	-15 min, 15 m/min	-5 min, 15m/min	-5 min, 15m/min	
								-3 min, 12 m/min	-5 min, 17 m/min	-5 min, 17 m/min	
								-2 min, 7m/min	-5 min, 15 m/min	-5 min, 15 m/min	
									-3 min, 12 m/min	-2 min, 7m/min	

segment, a period of 5 min. intervals, and a 5 min. cool-down.

Stage 1 consisted of 5 min at 7 m/min, 25 min at 12 m/min, and 5 min at 7 m/min for a total of 30 min. Stage 1 lasted one day.

Stage 2 consisted of one day of 5 min at 7 m/min, 20 min at 12 m/min, 5 min at 15 m/min, 5 min at 12 m/min, and 2 min at 7/min, totaling 37 min/day. After *Stage 2*, two days of training were lost to install better mouse containment and safety barriers. Only 7 and 5 min of training were performed on the respective lost days.

Stage 3 progressed across 3 days starting from 5 min at 7 m/min, to 5min at 12 m/min, to 10 min at 12 m/min, to 10 min at 15 m/min, to 10 at 12 m/min, to 3 min at 12 m/min, and to 2

min at 7 m/min, totaling 45 min/day. The final progression of *Stage 3* was at 5 min at 7 m/min, 5 min at 12 m/min, 45 min and 15 m/min, 3 min at 12 m/min, and 2 min at 7 m/min, totaling 60 min/day for 4 days. All training periods following stage 3 were 60 min.

Stage 4 consisted of 3 days of 5 min at 7 m/min, 5 min at 12 m/min, 35 min at 15 m/min, 5 min at 17 m/min, 5 min at 15 m/min, 3 min at 12 m/min, and 2 min at 7 m/min.

Stage 5 consisted of two days of 5 min at 7 m/min, 5 min at 12 m/min, 15 min at 15 m/min, 5 min at 17 m/min, 5 min at 15 m/min, 5 min at 17 m/min, 15 min at 15 m/min, 3 min at 12 m/min, and 2 min at 7 m/min. This was advanced to seven to nine days (depending on takedown) of 5 min at 7 m/min, 5 min at 12 m/min, 15 min at 15 m/min followed by 6 intervals of 5 min of 17 m/min and 5 min of 15 m/min with 3 min at 12 m/min, and 2 min at 7 m/min for a cool-down.

After training and the final GXT, animals were terminally anesthetized with 100mpk of sodium pentobarbital (Beuthanasia-D Special, Schering-Plough Animal Health Corp., Union, NJ). Upon complete non-responsiveness, animals were weighed and then euthanized by midline thoracotomy and removal of the heart. Upon removal, hearts were cleaned of fatty tissue, drained of blood, weighed, and frozen in liquid nitrogen. After euthanasia, left and right gastrocnemius (gastroc), plantaris, and soleus (sol) muscles were dissected, cleaned of connective tissue, weighed, and placed in cold Chappell-Perry buffer consisting of KCl (100 mM), MOPS (50 mM), EGTA (1 mM), EGTA (5 mM), MgSO₄·7H₂O (5 mM), and ATP (1 mM), pH 7.4 (with KOH). Complete tibialis anterior (TA) muscles were completely dissected, cleaned of connective tissue, weighted, frozen in liquid nitrogen, and stored for later analysis.

Respiration

Mitochondria were freshly isolated from ~200 mg of hindlimb tissue (combined 2 gastroc+plantaris and 2 sol) in cold Chappell-Perry buffer by standard differential centrifugation methods as previously described with minor modifications described in appendix I [136].

Oxidative phosphorylation rates in response to 125 μ M and 4 mM ADP were determined in freshly isolated mitochondria (75 μ g protein) using the two-channel high resolution respirometer (Oroboros Oxygraph; Innsbruck, Austria) with the saturating concentrations of the following substrate/inhibitor combinations in the provided order: pyruvate (5 mM) + malate (5 mM)--all respiratory measures, cytochrome *c* (10 μ M)--cytochrome *c* response, oligomycin (2 μ g/ml)--leak, and titrations of FCCP with an initial 1 μ l step of FCCP (0.5 μ M) followed by 0.5 μ l titrations--maximal respiration. After the pyruvate + malate addition, 125 μ M ADP was added to both chambers to achieve an initial state 3. Upon return to a stable baseline (state 4), 4 mM ADP was added to both chambers to achieve ADP saturation (state 3'). Respiration studies were performed at an initial oxygen concentration of 300 μ M at 37 °C in MiR06 respiration buffer containing EGTA (0.5 mM), MgCl₂·6 H₂O (3 mM), K-lactobionate (60 mM), taurine (20 mM), KH₂PO₄ (10 mM), HEPES (20 mM), sucrose (110 mM), 1 g/L BSA, 280 U/ml catalase, pH 7.4 (with KOH).

Protein Assay

The protein content of isolated mitochondria and homogenized TA were determined by BCA protein assay kit (Thermo Scientific; Rockford IL). Briefly, after isolation or homogenization, 10 μ l of diluted (1:100) isolate or homogenate were added in triplicate to a 96 well plate. BCA reagents A and B were combined in a 50:1 ratio and added (200 μ l) to all

sample wells. The plate was incubated at 37°C for 15 minutes. Absorbance at 562 nm was detected using a SpectraMax M2 Multi-Mode Microplate Reader using SoftMax Pro (Molecular Devices, LLC; USA). Protein concentrations were acquired in mg/ml.

Citrate Synthase Assay

A photometric kinetic absorbance assay for citrate synthase (CS) was performed in whole muscle homogenates as a marker to determine if mitochondrial biogenesis took place as a result of training, and later in isolated mitochondria as a rough index of TCA flux. Briefly, CS assay buffer was prepared with HEPES (20 mM), EGTA (1 mM), Sucrose (220 mM), and KCl (40 mM), pH 7.4 (with HCL) to make the CS reaction buffer with the addition of 200X DTNB (20 mM) and 100X AcetylCoA (10 mM). Reaction buffer was prepared in proportion to the number of samples to be run. 200 µl of reaction buffer were added to each well. Duplicate samples of 10 µl of 1:100 diluted TA homogenate or isolated mitochondria samples were added to the reaction buffer. Softmax Pro was prepared to read absorbance at 412 nm every 40 sec for 15 min with a 5 sec shake prior to the first read. The CS reaction was started by adding 10 µl of 1X oxaloacetate stock (1.1 mM) to each well, and the plate was quickly placed in the spectrometer. The average of the linear slope of the resulting data points was then divided by the protein content of the TA or isolated mitochondria to determine CS activity relative to protein content.

Lactate Dehydrogenase Assay

To establish a measure of SM lactate metabolism a photometric kinetic absorbance assay of LDH activity was performed. BioVision Inc. Lactate Dehydrogenase Activity Assay Kit substrates, buffers, standards, controls, and procedures were utilized (BioVision Incorporated,

Milpita, CA). Briefly, approximately 50 mg of frozen TA was homogenized 1:6 mass to volume (~250 μ l) in cold assay buffer with a glass homogenizer. Homogenate was centrifuged at 10,000 G for 15 min at 4°C. Homogenate supernatant was collected and the pellet discarded. In duplicate, 2 μ l of the samples were added to a 96 well plate and brought to 50 μ l with assay buffer. NADH standard was added in triplicate. NADH standard well volumes were brought to 50 μ l with assay buffer to yield 0, 2.5, 5.0, 7.5, 10, and 12.5 nmol/well standards. Once 50 μ l of reaction mix were added to each well, the plate was protected from light, and the plate was read every 5 min for 50 min at 450 nm at 37°C with Softmax Pro. The average linear slope of the change in absorbance was calculated and divided by TA protein content to determine LDH activity.

MCT1, UCP3, HNE, OXPHOS, and MnSOD Western Blotting

Mitochondrial content of MCT1 and UCP3 along with respiratory complexes 1-5 (OXPHOS), 4-hydroxynonenal-protein adducts (HNE), and manganese superoxide dismutase (MnSOD) were quantified with SDS-Page Western blotting to establish measures of potential lactate transport, uncoupling protein content, electron transport chain content, lipid peroxidation, and antioxidant defense. Proteins were probed using MCT1 (T-19) (Santa Cruz Biotechnology, Santa Cruz, CA; 1:500), UCP-3 (Abcam, Cambridge, MA; 1:850 and 1:500), OXPHOS antibody cocktail (Mitosciences, Eugene, OR; 1:2000), HNE-adducts (Calbiochem, Billerica, MA; 1:2000), and MnSOD (Assay Designs, Farmingdale, NY; 1:10,000). Isolated mitochondria used for OXPHOS and HNE blotting were first lysed and sonicated to disrupt mitochondria. To all samples, 7.5 μ l of 2X Laemmli loading buffer was combined with a quantity of autoclaved water and isolated mitochondria determined by protein content; 30 μ g of protein were used for

UCP3, MCT1, and HNE while 5 μ g were used for OXPHOS and the corresponding MnSOD probe. The prepared samples were frozen overnight and then heated in a heat block at 100°C for 10 min; OXPHOS and HNE samples were heated at 37°C for 10 min. The ladder (Western C Standards) (7 μ l) and samples (15 μ l) were loaded into precast gels (Bio-Rad, Hercules, CA) and run at 100 V until protein bands lined up at the edge of the stacking gel, then the gel was run at 200 V for ~1 hr. After 1 hour the gel was removed and carefully sandwiched with a nitrocellulose membrane in a horizontal transfer set up. The apparatus was filled with transfer buffer and placed in ice pack and run at 100 V for 1 hr. The starting amperage was between 0.5 and 0.7 A. After the transfer, the membrane was stained with Ponceau to ensure transfer and assist in membrane trimming.

After rinsing, the membranes were blocked with 5% non-fat dry milk (NFDM) in TBST for 1 hr. After blocking the respective primary antibodies were applied overnight in 5% NFDM. Bound membranes were washed with TBST 6 times for 5 min. Secondary antibodies were applied for 1 hr (UCP3, goat anti-rabbit—1:500; MCT1, horse anti-goat—1:500; HNE, goat anti-mouse; OXPHOS and MnSOD, goat anti-rabbit—1:2000; ladder, Stepactin AP (Bio-Rad, USA)—1:5000) with 1% NFDM in TBST. After secondary antibody application, membranes were washed 6 times with TBST for 5 min and briefly with 1X TBS.

After washing, bound membranes were covered with Immune-Star AP Substrate (Bio-Rad, USA) solution. Membranes were then imaged using VisionWorks (UVP Inc., Upland, CA). Following UV imaging, BCIP®/NBT-Blue (Sigma-Aldrich, St. Louis, MO) was applied to membranes until bands appeared then membranes were imaged on a flatbed scanner (Epson Perfection V500 PhotoScanner, Epson, Long Beach, CA). After MCT1, HNE, and OXPHOS imaging, membranes were stripped using Restore™ PLUS Western Blot Stripping Buffer

(Thermo Scientific, Rockford, IL) for 5 min. After stripping, the membranes were washed with TBST 6 times for 5 min and the membrane blocking and antibody application procedures were repeated with the UCP3 primary antibody on the MCT1 blots and MnSOD on the HNE and OXPHOS blots. After application and washing of the secondaries, NBT-Blue was applied. Membranes were imaged again. Following the NBT-Blue imaging, the membranes were stained for ~1 min with 0.1% (w/v) Naphthol Blue Black (Santa Cruz Biotechnology, Santa Cruz, CA) in 25% (v/v) isopropanol then destained for ~30 min with 5% acetic acid [137]. Membranes were then imaged to quantify protein loading. Protein content was normalized to TazS Naphthol stain or WTS for OXPHOS complexes. All images were analyzed using ImageJ software (NIH).

Statistics and analysis

Effects of mouse genotype and exercise were analyzed using a two-way univariate ANOVA (SPSS, Chicago, IL). P values ≤ 0.05 were considered significant. Results are displayed as means \pm SE.

CHAPTER IV

RESULTS

Anthropometrics.

Anthropometric results are displayed in Table 2. Exercise training produced no significant difference ($P = 0.330$) in body weight between sedentary and trained animals; however, *taz* mice were significantly smaller than WT mice ($P = 0.000$). Hindlimb and TA masses followed similar genotype-correlated differences with no effect of exercise. Exercised *taz* mice had significantly heavier hearts ($P = 0.025$) than sedentary *taz* mice. This trend continued after adjusting heart mass to body mass. Additionally, relative to body mass, exercised hearts were significantly larger than sedentary hearts ($P = 0.023$). Relative to body mass, *taz* hearts were significantly larger than WT hearts ($P = 0.001$). This relationship and the exercise relationship were primarily driven by TazX hearts.

Table 2. Anthropometric characteristics of experimental mice (n = 15 WTS, 8 WTX, 11 Tazs, 8 TazX).

	WTS	WTX	TazS	TazX	Genotype (P)	Exercise (P)	TazS v TazX (P)	WTS v WTX (P)	WTS v TazS (P)	WTX v TazX (P)
Body Weight (g)	25.54±0.76	24.51±1.07	21.52±0.76*	20.66±1.00*	0.00	0.33	0.50	0.48	0.00	0.01
Heart Weight (mg)	112.06±4.45	111.86±5.83	105.92±4.28	122.13±5.45*	0.69	0.12	0.03	0.98	0.32	0.21
Heart Weight : Body Weight (mg/g)	4.51±0.21	4.63±0.3	4.90±0.20	5.92±0.25*	0.00	0.02	0.01	0.75	0.19	0.00
Combined Hindlimb Weight (mg)	268.43±6.46	272.00±8.54	236.71±6.46*	233.25±8.54*	0.00	0.99	0.75	0.74	0.00	0.00
Combined TA (mg)	131.33±4.09	126.33±5.79	102.82±3.78*	108.75±5.00*	0.00	0.92	0.35	0.48	0.00	0.03

Data are mean ± SE.

GXT Performance.

Taz mice ran significantly shorter during the pre-training GXT ($P = 0.000$); *Taz* mice ran for ~40% the time of WT mice. *TazX* mice ran significantly longer in the post-test than the *TazS* mice ($P = 0.000$). However, *TazX* mice still ran for a significantly shorter time than the WT mice ($P = 0.002$) (Table 3 and Figure 1). The percent change or improvement between *TazX* and *TazS* mice was not significant ($P = 0.099$) (figure 1). Due to the ceiling on the test, performance differences between WTS and WTX could not be determined.

Table 3. GXT performance parameters

	WTS	WTX	TazS	TazX	Genotype (P)	Exercise (P)	TazS v TazX (P)	WTS v WTX (P)	WTS v TazS (P)	WTX v TazX (P)
Pre-Test GXT (s)	1649.5±125.3	1713.4±88.6	642.8±125.3*	825.5±88.6*	0.00	0.27	0.25	0.68	0.00	0.00
Post-Test GXT (s)	1785.5±87.3	1792.1±61.7	947.5±87.3*	1485.5±61.7*	0.00	0.00	0.00	0.95	0.00	0.00
GXT change (s)	136.0±138.5	78.6±97.9	304.8±138.5	660.0±97.9*	0.01	0.23	0.05	.739	0.40	0.00
% Change	9.069±23.607	7.388±16.693	49.109±23.607	99.188±16.693*	0.00	0.25	0.10	0.95	0.24	0.00

Data are mean ± SE.

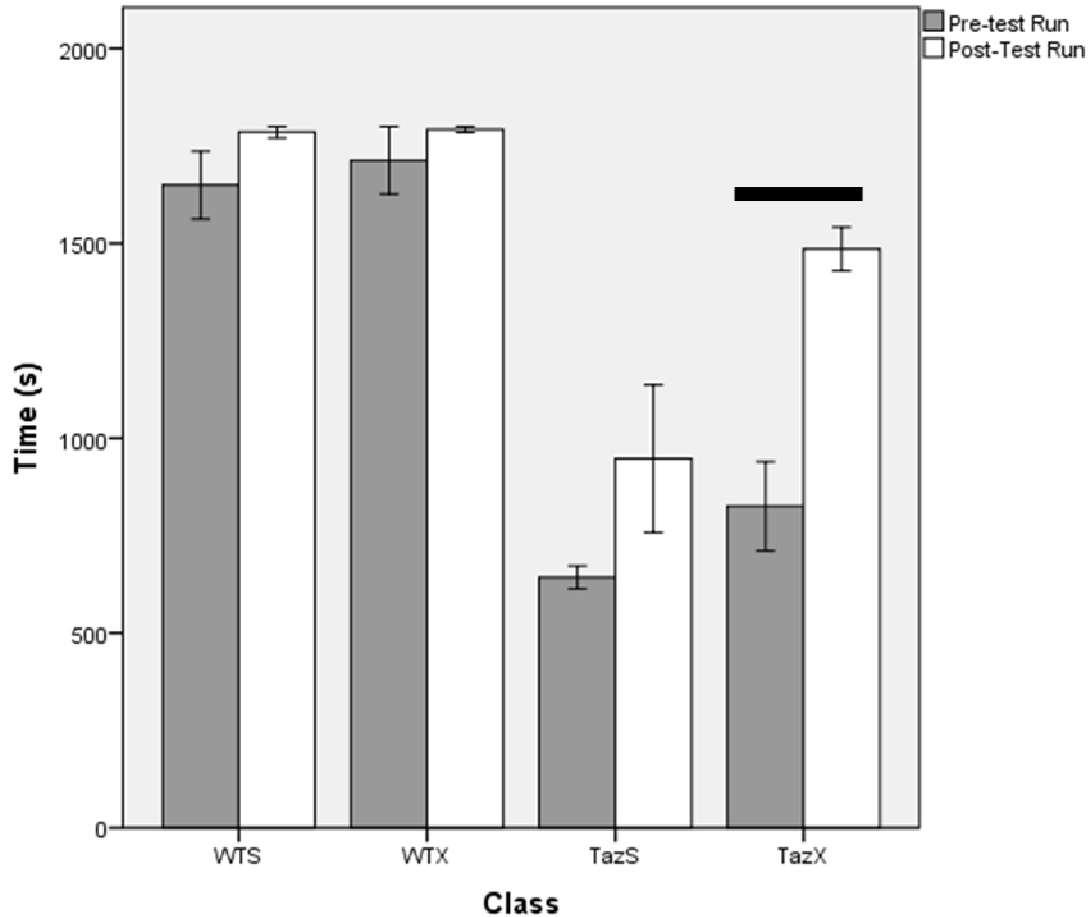


Figure 1. GXT running time in s. There were no significant differences within genotype groups in the pre-test. TazX mice ran for significantly longer post-taining. Horizontal bar indicates significant ($P < 0.05$) increase in running time in TazX. Data are mean \pm SE.

Lactate Dehydrogenase Activity.

Kinetic spectrophotometric assays for lactate dehydrogenase activity indicated significantly decreased muscle LDH activity in exercised mice ($P = 0.003$). This effect was primarily due to the significant difference between WTS and WTX (WTS: 0.903 ± 0.123 mU/ml; WTX: 0.229 ± 0.157 mU/ml) ($P = 0.002$). The two *taz* groups did not have significantly different LDH activity ($P = 0.289$), and TazX mice were not significantly different from WTX mice.

Sedentary *taz* mice (0.464 ± 0.118 mU/ml) had significantly lower LDH activity than sedentary WT (0.903 ± 0.123 mU/ml) ($P = 0.014$) (figure 2).

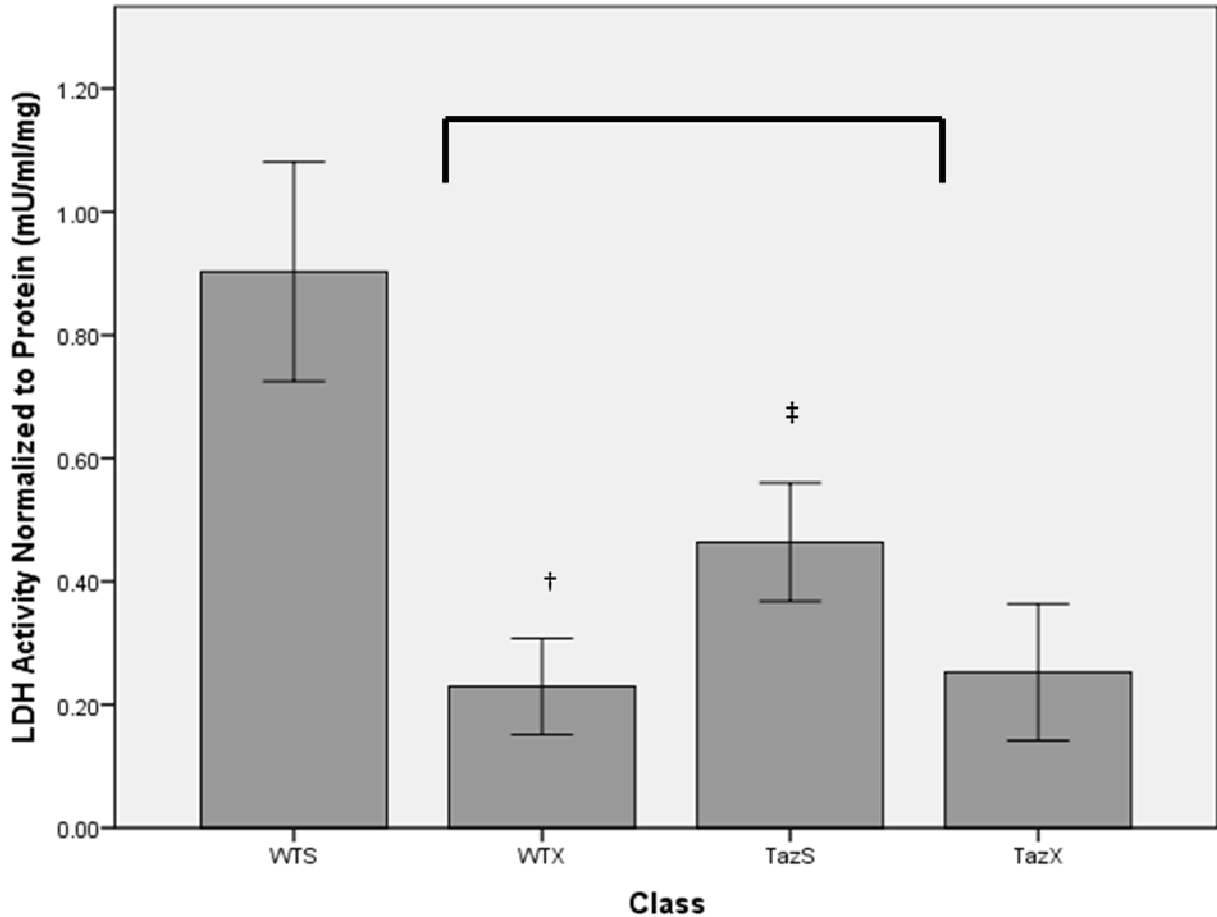


Figure 2. Lactate dehydrogenase levels. Exercised animals had significantly lower LDH activity. The TazS and WTX mice had significantly lower LDH activity than WTS. Bracket indicates a significant ($P \leq 0.05$) effect of exercise † $P \leq 0.05$ WTS vs. WTX, ‡ $P \leq 0.05$ WTS vs. TazS. Data are mean \pm SE.

Citrate Synthase Activity

In homogenized TA, CS activity assessed by kinetic photometric assay was significantly elevated with exercise ($P = 0.047$) (figure 3). Although, when WTX and TazX were compared separately to sedentary controls, exercise had no significant effect on CS activity. Within isolated

mitochondria, citrate synthase activity trended toward a decrease with exercise ($P = 0.081$) (figure 4).

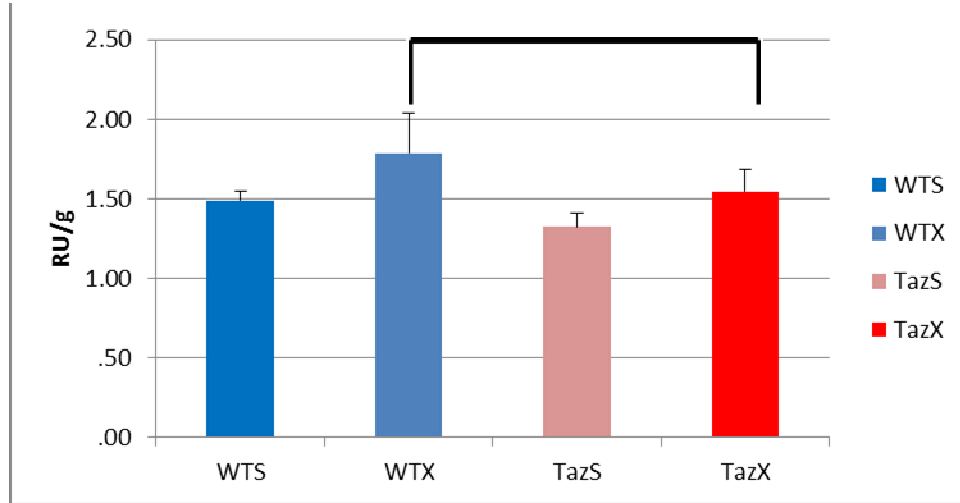


Figure 3. Skeletal muscle (TA) citrate synthase activity. Within homogenized SM, exercised animals had significantly greater CS activity. Bracket indicates a significant ($P \leq 0.05$) effect of exercise. Data are mean \pm SE.

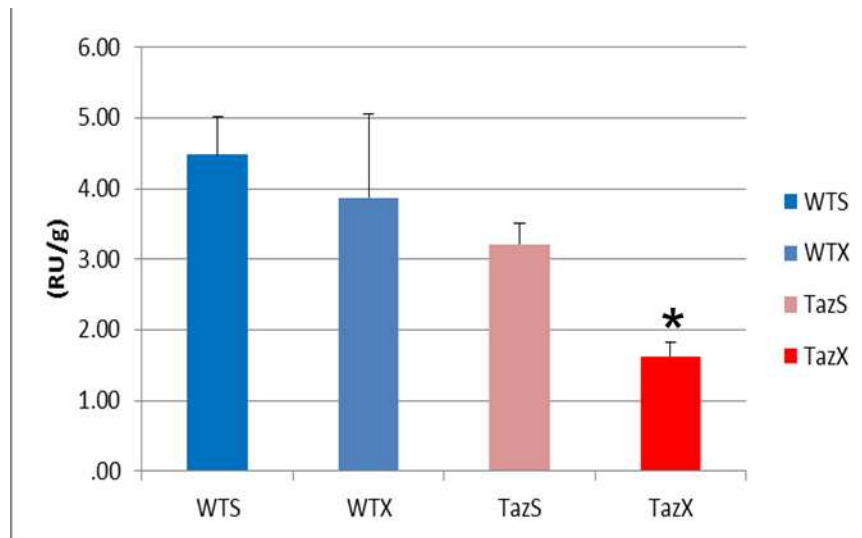


Figure 4. Mitochondrial citrate synthase activity. TazX mice had significantly lower CS activity within the isolated mitochondrial fraction than TazS. * $P \leq 0.05$ TazS v TazX. Data are mean \pm SE.

This difference was primarily due to TazX CS activity being nearly half that of TazS (TazX: 1.629 ± 0.692 RU/g; TazS: 3.211 ± 0.543 RU/g; WTS: 4.484 ± 0.505 RU/g; WTX: 3.871 ± 0.692 RU/g) ($P = 0.079$ vs. $P = 0.479$). Further contrasting with TA CS activity, *taz* mice had significantly lower CS activity than WT mice in isolated mitochondria fractions ($P = 0.007$).

Mitochondrial Respiration Parameters.

High resolution respirometry was used to establish measures of functional mitochondrial capacity in response to *taz* genotype and exercise. Neither training nor genotype affected state 2 respiration. State 3 achieved with a non-saturating titration of ADP ($125 \mu\text{M}$) produced a significantly greater response in the WT mice than in *taz* mice ($P = 0.000$). The ensuing state 4 was significantly lower in the *taz* mice ($P = 0.032$), and exercised mice had significantly lower state 4 respiration than sedentary mice ($P = 0.003$). TazS mice did have significantly lower state 4 than WTS mice ($P = 0.053$), but TazX and WTX mice were not significantly different ($P = 0.196$). State 3' (respiration with saturating ADP; 4 mM) was significantly lower in *taz* and exercised mice ($P = 0.00$ and 0.015 , respectively). However, as separate groups TazX and WTX only trended to being lower than TazS and WTS ($P = 0.084$ and 0.079 , respectively). Cytochrome *c* response was not significantly elevated above State 3' between groups, but there was a trend toward a lower elevation in trained animals ($P = 0.058$). Exercise trained animals as a group also had significantly lower rates of respiration when subjected to oligomycin than sedentary animals ($P = 0.007$) with WTX being significantly lower than WTS, but TazX only trended to be lower than TazS ($P = 0.037$ and 0.069 , respectively). FCCP respiration rates were significantly lower in *taz* and exercise groups ($P = 0.000$ and 0.005 respectively). Both TazX and

WTX FCCP respiration rates were significantly lower than their respective controls' ($P = 0.044$ and 0.038 , respectively), and both TazX and TazS groups had lower FCCP rates than their WT controls ($P = 0.000$ and 0.010 , respectively). Table 4 shows respirometry data, which are graphically broken down in Figure 5.

Table 4. Summary of respirometry data.

	WTS	WTX	TazS	TazX	Genotype(P)	Exercise(P)	TazS v TazX (P)	WTS v WTX (P)	WTS v TazS (P)	WTX v TazX (P)
State2 (pmol/(s*mg))	739.136±195.775	839.614±139.528	754.453±101.697	533.541±139.528	0.35	0.57	0.23	0.63	0.85	0.20
State 3 (D = 125mM) (pmol/(s*mg))	4089.776±344.923	4050.420±496.976	2623.050±362.940	436.576±496.976	0.00	0.37	0.23	0.95	0.01	0.00
State4 (pmol/(s*mg))	1915.87±129.079	1398.639±195.149*	1846.97±133.312*	1047.536±162.545*	0.03	0.00	0.03	0.03	0.05	0.20
State 3' (D = 4mM) (pmol/(s*mg))	4992.59±1371.348	3779.672±561.425	2379.593±383.526*	1827.548±525.165*	0.00	0.02	0.09	0.09	0.00	0.01
Cytochrome c (pmol/(s*mg))	5449.45±401.356	4570.218±595.276	3154.974±434.728	1866.839±595.176	0.00	0.04	0.09	0.23	0.00	0.00
Cytochrome c-State 3 change(pmol/(s*mg))	336.195 ±72.596	116.789 ±109.755	176.470 ±74.977	39.291 ±102.566	0.20	0.06	0.29	0.13	0.13	0.61
Cytochrome C% Change of State 3	7.53±1.570	3.242 ±2.373	3.359 [#] ±1.621	2.470 ±2.220	0.56	0.06	0.21	0.14	0.50	0.81
Oligomycin(pmol/(s*mg))	726.62±72.733	399.758±31.122*	421.077±67.771*	395.938±99.119*	0.88	0.01	0.07	0.04	0.20	0.98
Vmax -CCP (pmol/(s*mg))	5205.155±389.171	3693.947±568.372	2932.077±401.931	1516.134±550.371	0.00	0.00	0.04	0.04	0.00	0.01

Data are mean ± SE.

When maximal leak rates were normalized to maximal oxidative phosphorylation rates (L/P—Oligomycin/cytochrome *c*—maximal phosphorylation rate), *taz* mice had significantly greater rates of oligomycin induced leak relative to the maximum achieved respiration rate ($P = 0.051$) (Figure 6). This relationship was primarily attributable to the difference between TazS and WTS ($P = 0.043$). Respiratory control ratios (RCR) defined by State 3 to State2 and State 3 to State 4 can be used as a measure of the phosphorylation control of mitochondrial respiration: the higher an RCR the better a mitochondria can increase respiration above baseline/background in the presence of ADP. *Taz* mice had significantly lower 3/2 and 3/4 RCR ratios ($P = 0.000$; 3/4: $P = 0.000$), indicating that *taz* mice are less capable of increasing state 3 relative to state 2 (Figure 7).

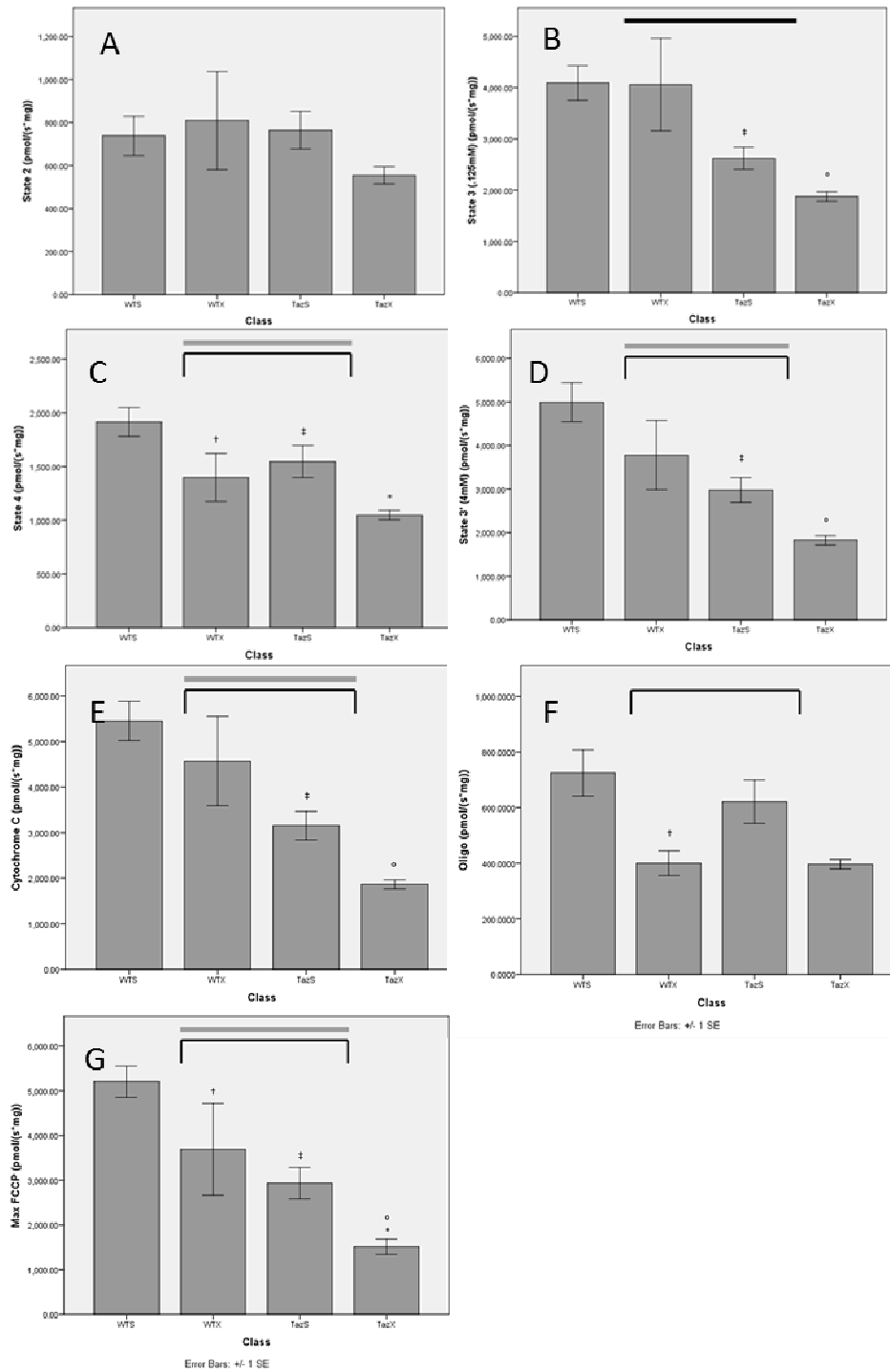


Figure 5. Breakdown of individual respiratory measures. A) State 2. There were no differences between groups. B) State 3 (125 μ M ADP). *Tac* mice had a significantly lower state 3 than WT mice. C) State 4. There was a significant decrease in state 4 respiration with exercise and the *tac* genotype. D) State 3' (4mM ADP). Exercise and genotype significantly lowered state 3'. E) Cytochrome *c*. Exercise and genotype significantly lowered state cytochrome *c* response. F)

Response to oligomycin inhibition. Exercise significantly lowered oligomycin respiration. G) Maximal achieved respiration with titrations of FCCP. Exercise and genotype significantly lowered maximal FCCP respiration. Horizontal bars indicate significant ($P \leq 0.05$) genotype effect. Brackets indicates a significant ($P \leq 0.05$) exercise effect. * $P \leq 0.05$ TazS v TazX, † $P \leq 0.05$ WTS v WTX, ‡ $P \leq 0.05$ WTS v TazS, ⁰ $P \leq 0.05$ WTX v TazX. Data are mean \pm SE.

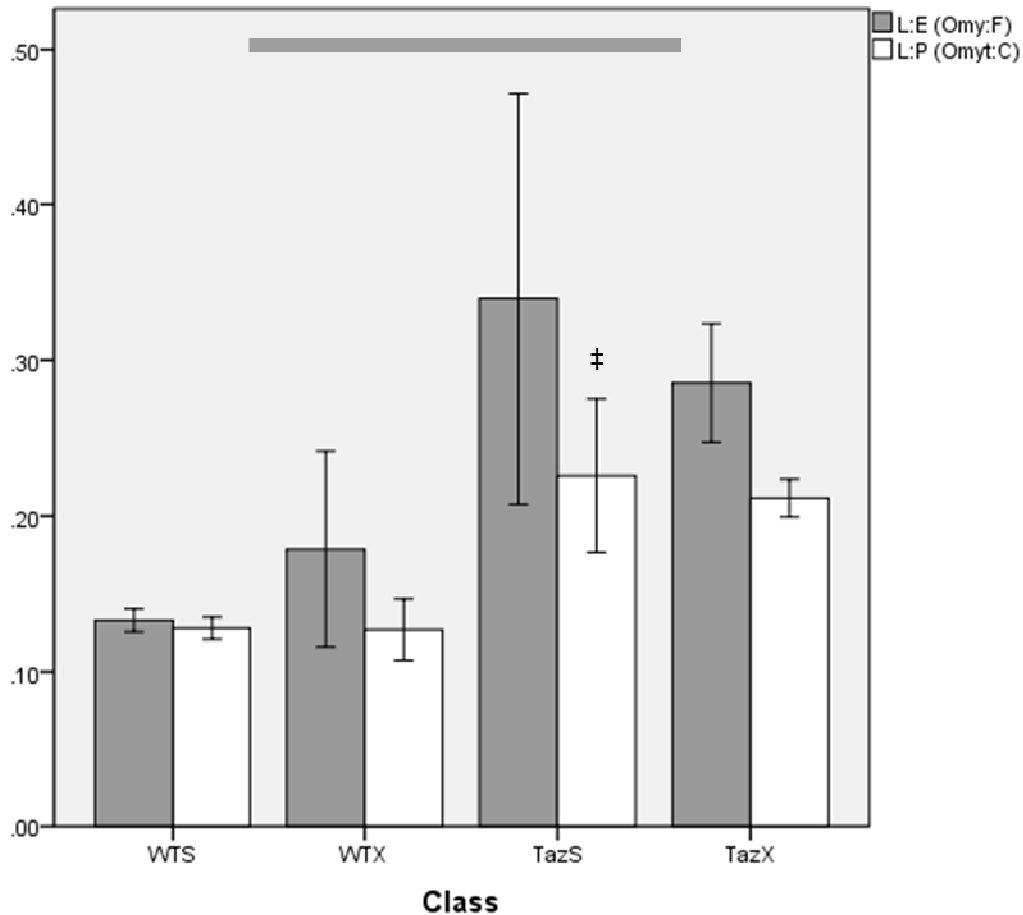


Figure 6. Ratios demonstrating different measures of maximal respiration to leak. Genotype significantly increased mitochondrial leak as assessed by either L:E or L:P. Horizontal grey bar, $P \leq 0.05$ for genotype interaction with L:P, ‡ $P \leq 0.05$ WTS v TazS. Data are mean \pm SE.

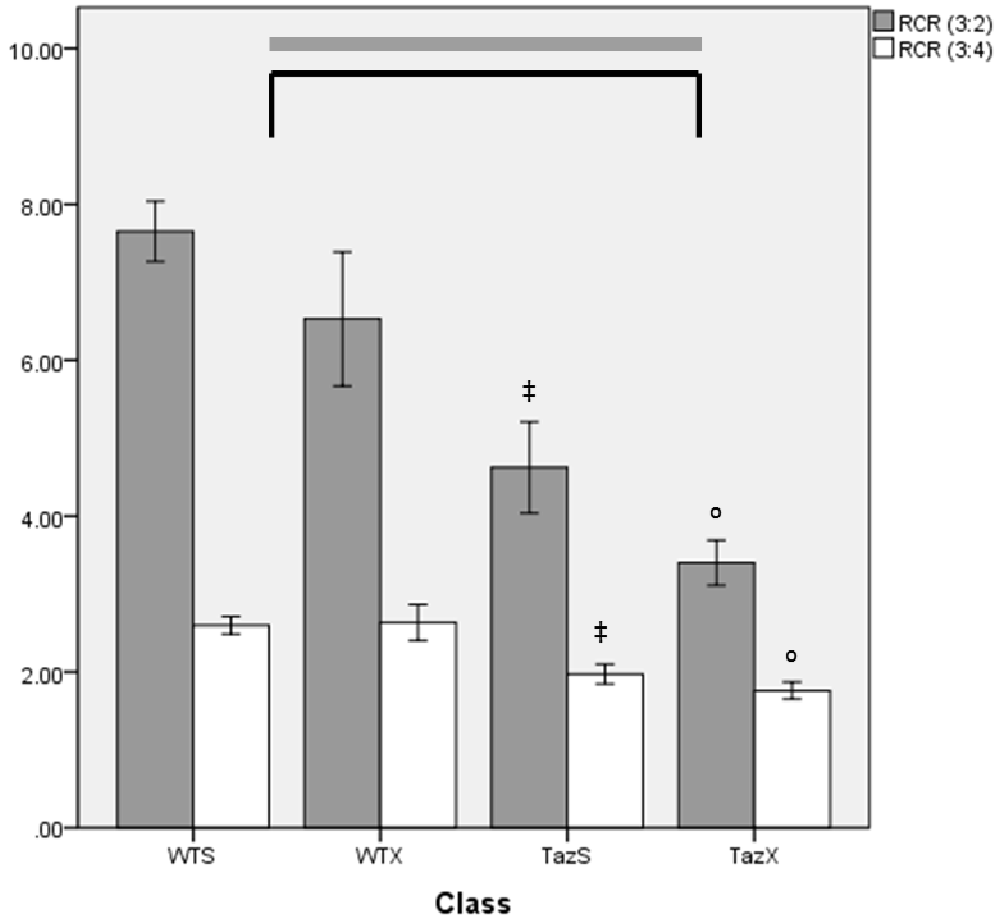


Figure 7. Ratios of respiratory control or capacity to increase respiration above background. Genotype and exercise produced significantly less coupled mitochondria as assessed by state 3:2 or 3:4. Horizontal bar indicates significant ($P \leq 0.05$) genotype effect with 3:2. Brackets indicates a significant ($P \leq 0.05$) exercise effect in 3:2. ‡ $P \leq 0.05$ WTS v TazS, ° $P \leq 0.05$ WTX v TazX. Data are mean \pm SE.

Mitochondrial Proteins.

Uncoupling protein 3 levels quantified by SDS-Page Western blotting normalized to TazS revealed no significant changes in UCP3 with exercise ($P = 0.616$); however, UCP3 levels were significantly depressed in *taz* mice ($P = 0.005$). When the relative means of UCP3 and mitochondrial CS to TazS are compared there was a significant effect of exercise to increase UCP3 to mitochondrial CS (WTS: 1.26 ± 0.22 , WTX: 2.32 ± 0.29), TazS: 1.14 ± 0.23 , TazX:

2.32 ± 0.29, $P = 0.000$). MCT1 protein, relative to TazS levels, was not significantly affected by exercise ($P = 0.641$) but was significantly lower in *taz* mice ($P = 0.017$). Mitochondrial MCT1 and UCP3 proteins normalized to TazS are displayed in figure 8.

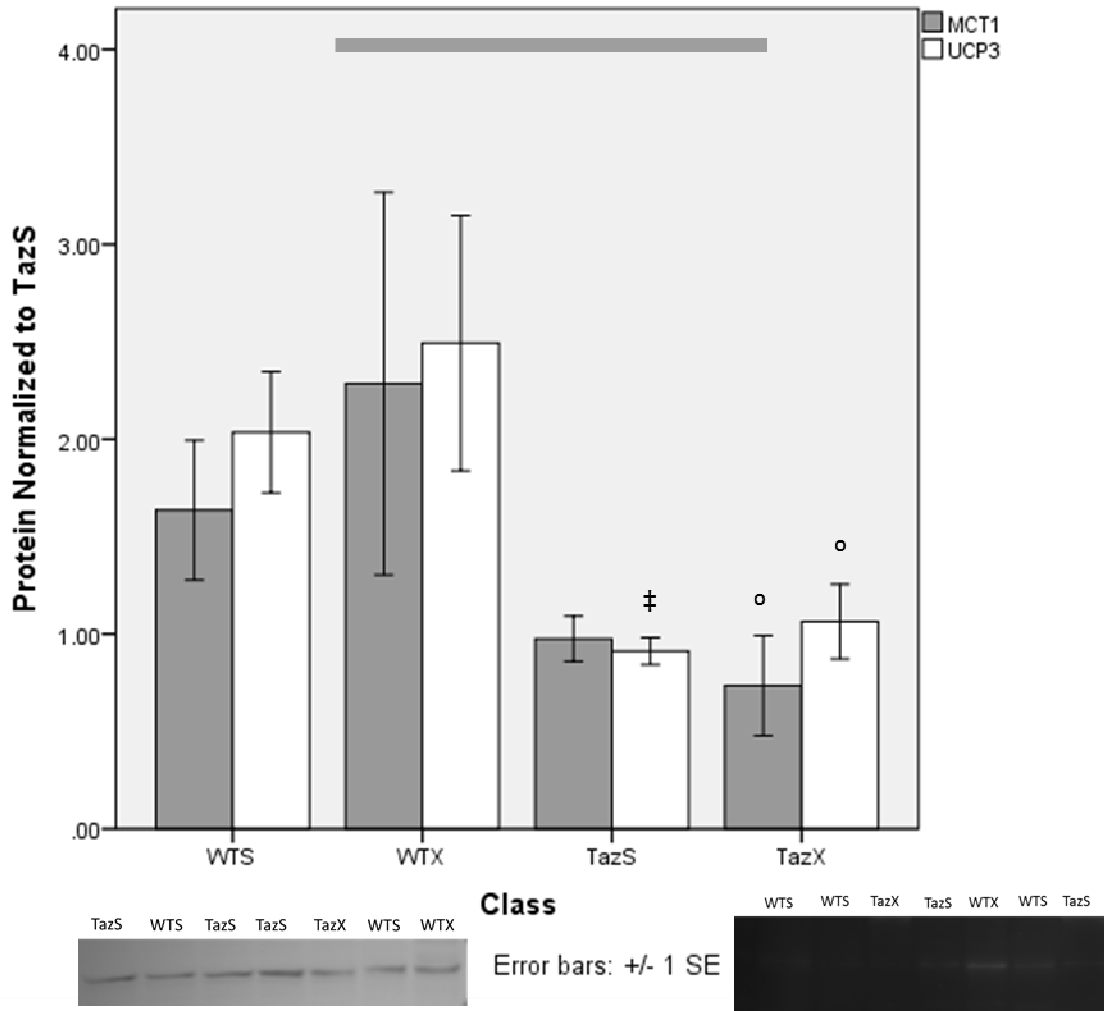


Figure 8. Mitochondrial MCT1 and UCP3 normalized to TazS protein. The left blot is a representative blot of UCP3. The right blot is a representative blot of MCT1. *Taz* mice had significantly less MCT1 and UCP3 than WT counterparts. Horizontal bar indicates significant ($P \leq 0.05$) genotype effect with UCP3. ‡ $P \leq 0.05$ WTS v TazS, ° $P \leq 0.05$ WTX v TazX. Data are mean ± SE.

Examination of OXPHOS tentatively revealed a significant reduction in Complex 1 in *taz* mice ($P = 0.030$); However, Complex 1 data appeared to be more variable than other OXPHOS proteins. No discernible bands were detected for complex 2. Complexes 3 and 4 were not

significantly affected by genotype or exercise, and this trend remained when all complexes were summed (Figure 9).

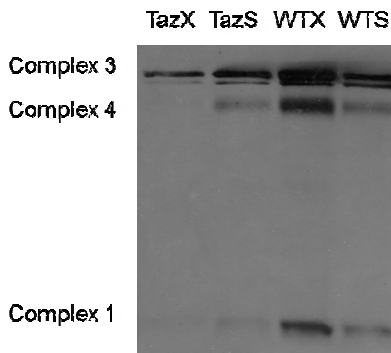
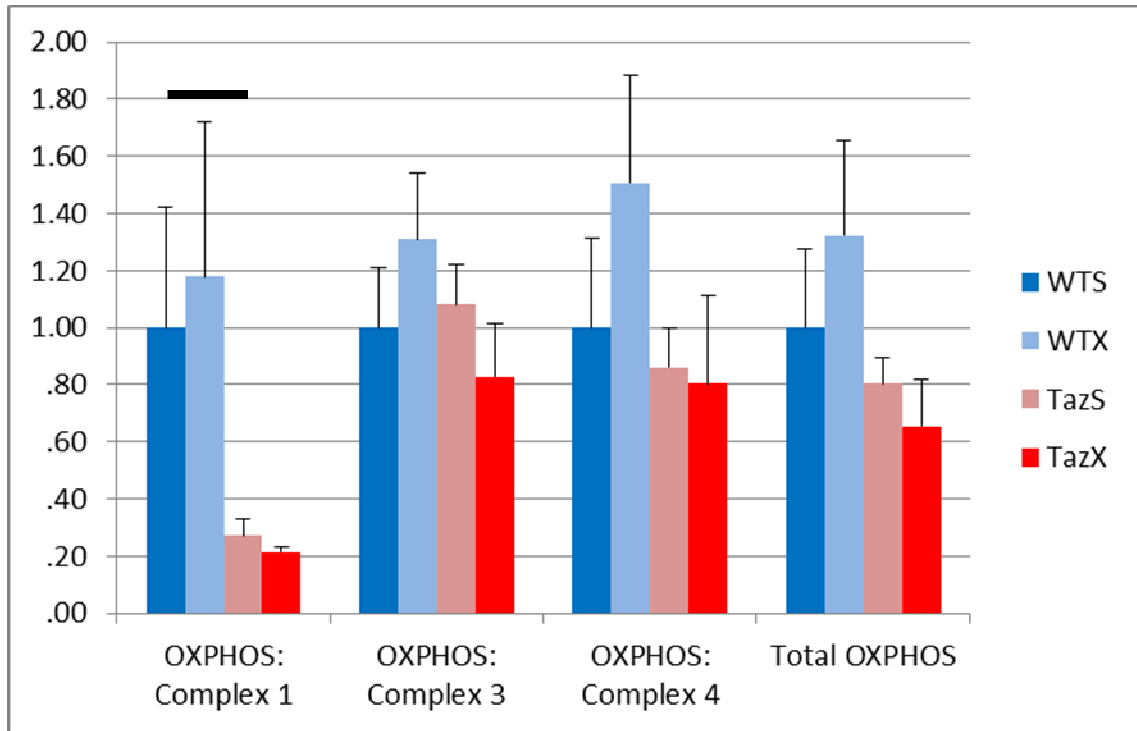


Figure 9. OXPPOS protein normalized to WTS. Representative blot of OXPPOS with complexes indicated. *Taz* mice had significantly lower complex 1 protein than WT mice. Horizontal bar indicates significant ($P \leq 0.05$) genotype effect within complex 1. Units are relative absorbance to WTS. Data are mean \pm SE.

HNE levels were examined as a measure of oxidative stress, and, despite a trend toward lower HNE in *taz* mice ($P = 0.062$), HNE levels were not significantly altered by genotype or training (figure 10). MnSOD levels were examined in parallel with HNE to test a measure of

ROS mitigation. MnSOD levels were not significantly different between sedentary and exercised mice. *Taz* mice did have significantly lower levels of MnSOD ($P = 0.012$) (figure 10). However, when the relative means of MnSOD and mitochondrial CS to TazS were compared as a ratio there was a trend for elevated MnSOD levels (WTS: 1.10 ± 0.32 , WTX: 1.55 ± 0.28 , TazS: 1.29 ± 0.28 , TazX 1.82 ± 0.28 , $P = 0.11$).

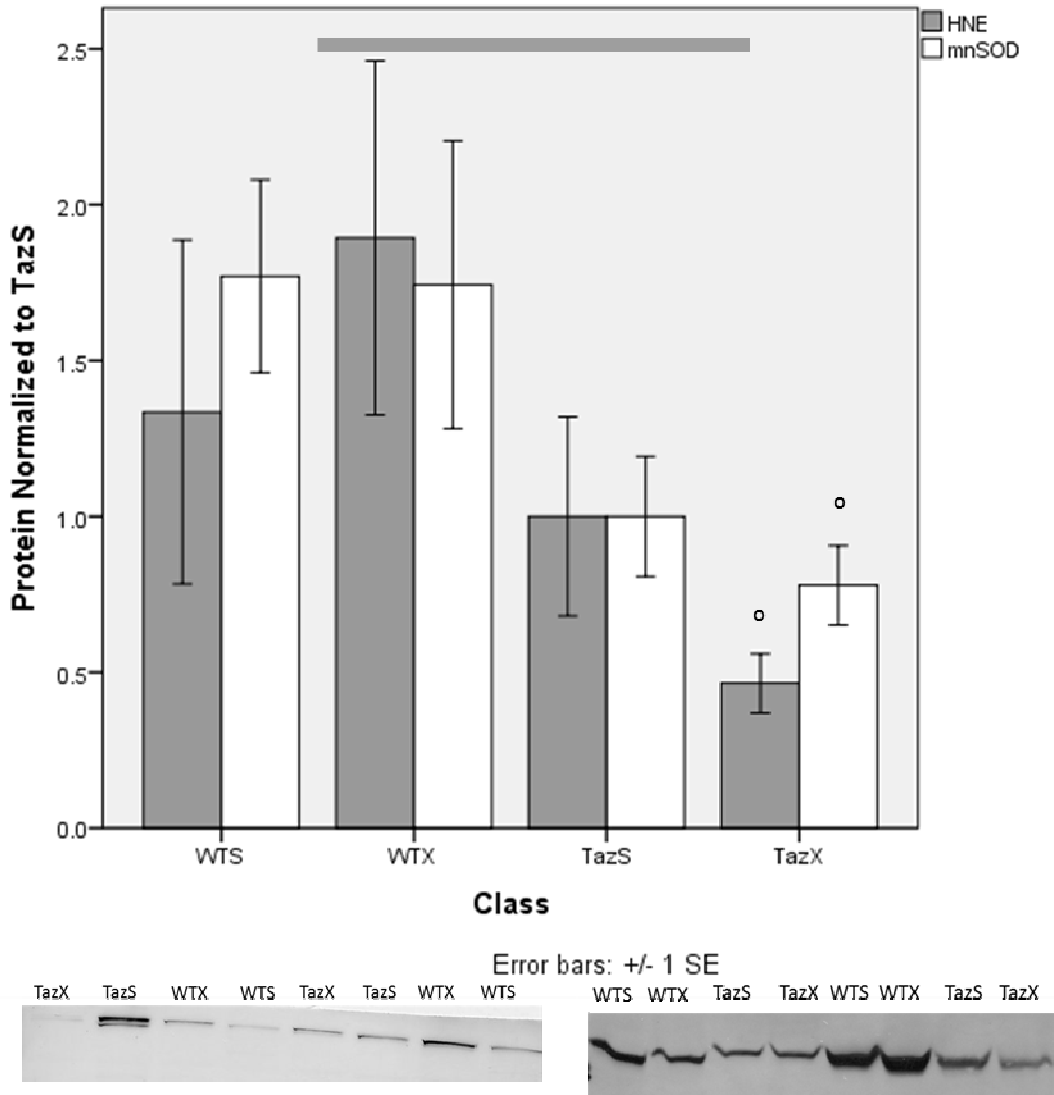


Figure 10. HNE and MnSOD protein normalized to TazS. Left blot is representative of HNE. *Taz* mice had significantly lower MnSOD and HNE levels. Right blot is representative of MnSOD. Horizontal bar indicates significant ($P \leq 0.05$) genotype effect within MnSOD. ^o $P \leq 0.05$ WTX v TazX. Data are mean \pm SE.

CHAPTER V

DISCUSSION

This study sought to characterize the response to exercise of *taz* mice and Taz deficient SM mitochondria using a progressive exercise training program. Initially it was hypothesized that exercise would improve exercise capacity, perhaps by increasing SM LDH activity (errant initial hypothesis) with a concomitant increase in MCT1, elevated UCP3, increased mitochondrial biogenesis, and a possible recovery of diminished mitochondrial respiration. Later measures of HNE, OXPHOS, and MnSOD were added to interpret some of the emergent findings.

Exercise Performance.

The initial GXT confirmed exercise intolerance in the *taz* mouse, and exercise intolerance was abetted by exercise training. The significant improvement in TazX GXT times indicates that the applied training stress was adequate to overload, but not exhaust *taz* mice. The applied training speed and duration were similar to other studies that have shown improvement with exercise in other diseased mouse models, and the selected speed intervals corresponds with speeds (15-18 m/min) that elicit a maximal lactate steady state or ~65% of VO_{2max} [135, 138-140]. Whether the training program enhanced WTX performance or not could not be determined due to the ceilinged GTX. However, the primary purpose of this study was to characterize the *taz* mouse response to exercise, and exercising the WTX at the same absolute intensity potentially magnifies the differences in adaptation between *taz* and WT mice. Changes in state 3' and

significant decreases in state 4 and LDH provides evidence that WTX mice did experience some degree of exercise adaptation.

Increased absolute and relative heart mass may have contributed to the improved exercise capacity of the TazX mice [14]. Because mice were not subjected to echocardiography, whether this adaptation was the result of dilated cardiomyopathy or beneficial adaptation remains to be determined. Other factors such as, but not limited to, economy, hematocrit, capillary density, fiber type change, or biomechanical changes also were not assessed, but could have also contributed to the increased exercise performance. TazX mice did appear to have a slightly less splayed running form than the TazS mice, suggesting better biomechanical efficiency, but this was not quantified beyond casual observations.

Decreased Lactate Dehydrogenase Activity.

LDH activity was expected to increase with exercise because lactate utilization and clearance increase with exercise. The significant decrease in LDH activity with exercise was surprising, but these findings are consistent with the literature on rodent SM LDH activity. Previous work has shown decreased LDH activity in rodent SM, but the decrease in LDH activity is accompanied by a shift in LDH isoform to one favoring lactate conversion to pyruvate [50-53]. It is also likely that an overall increased oxidative capacity reduced the production of and reliance on lactate within SM.

These data alone are inadequate to definitively demonstrate whether or not the enhanced exercise capacity of *taz* mice can be attributed to a compensatory reliance on and enhancement of glycolytic metabolism, but the similar LDH activity rates in WTX as in TazX do not support

this notion. Also, the decrease in MCT1 would not support an increased reliance on glycolytic metabolism. In that sedentary *taz* mice also had significantly lower LDH activity may be evidence of a stressed metabolic state in *taz* mice, in that they partially resemble an exercised animal.

Uncoupling Protein 3.

Due to the duration and low-intensity of the training, no change or some increase in UCP3 would have been expected [32, 34, 38, 107], and indeed there was no significant effect of training on UCP3. There was also no evidence of increased uncoupling due to exercise, as demonstrated by the lack of significant change in L/P. However, a ratio of the relative means (to TazS) of UCP3 and mitochondrial CS reveals a significant effect of exercise to increase the ratio to UCP3 to mitochondrial CS. This ratio, although a rough measure, indicates an enhanced ability of mitochondria to increase proton flux in proportion to proton creation. In light of the insignificant changes in leak, it is possible to UCP3 facilitated moderation of proton flux may only be detectable when fat is used as a substrate.

“Mitochondrial Biogenesis,” Respiration, and Oxidative Stress.

Based on CS assay results of the TA, there was an increase in mitochondrial content per mg of SM tissue with exercise. This comports with most previous observations [25-28, 30, 74, 75]. However, the significantly lower CS in the isolated mitochondria of *taz* mice relative to WT mice and the trend toward lower CS in isolated mitochondria with exercise indicates that CS was

decreased per a unit of mitochondria in *taz* mice and potentially as an effect of exercise as well. Lower CS per mg mitochondrial protein implies a lower capacity to generate NADH, via decreased substrate delivery to the TCA cycle, which could contribute to the impaired respiration observed in *taz* and WTX mice. Rather than being a maladaptation to exercise, lower mitochondrial CS may point to a ROS mitigating adaptation to exercise discussed below.

In *taz* mice, impaired cristae formation appears to selectively diminish complex 1 subunit proteins, either by impairing mitochondrial import and/or assembly of the complex subunits and/or inducing adaptive downregulation or proteolysis of existing subunits. The impaired observed respiratory capacity, although not made directly of complex 1, is consistent with a significant decrease of complex 1 relative to WT mice; these observations are also consistent with other unpublished proteomics data from our lab, which show a 20-70% decrease in complex 1 in *taz* heart mitochondria as well as 20% lower cardiac nicotinamide levels compared to WT mice. Impaired cristae formation and low complex 1 protein likely contribute to the dysfunctional electron transport complex (ETC) observed during mitochondrial respiration in the *taz* mice. Downregulated CS levels per mitochondria may actually mitigate ROS production by preventing an overabundant pressure of NADH and electrons through complex 1 and further downstream at complex 3, which are the predominant sites of mitochondrial ROS generation [141]. Decreased CS may therefore decrease a damaging flux of electrons through an impaired ETC.

Mitochondria CS downregulation may also maintain a more metabolically favorable NAD⁺/NADH ratio to support continued oxidative metabolism. An overabundance of NADH will not only promote ROS production at complexes I and III, but it ties up NAD⁺, and limits its availability to TCA cycle enzymes, pyruvate dehydrogenase and β -oxidation. Downregulation of

NADH production may seem problematic during the increased metabolic demand of exercise, but the increased metabolic demand of exercise increases mitochondrial expansion within tissue as was seen with the significantly greater muscle tissue CS levels in exercised mice. Therefore, with increased mitochondrial biogenesis, high metabolic demand can be met while a concomitant reduction in CS per mitochondria permits maintenance of energy production and provides protection against oxidative damage.

To verify that oxidative damage was actually mitigated, mitochondrial proteins were probed for HNE. HNE was significantly lower in TazX mice than TazS mice. To determine whether the lower HNE levels were due to increased mitochondrial antioxidant capacity, blots for MnSOD were run. MnSOD levels were not significantly different between exercised mice and sedentary controls. The elevated ratio of the relative means MnSOD to mitochondrial CS with exercise possibly indicates another level of ROS protection in response to the backlog of NADH in the matrix associated with the increased metabolic demand of exercise. These data support that case that the observed decreases in mitochondrial CS may have been a function of selective mitochondrial remodeling in response to exercise that limits the flux of electrons through the TCA and the ETC in order to mitigate ROS production while at the same time increased ATP demands can be met by increased mitochondrial biogenesis.

Conclusion.

Exercise training partially recovers exercise impairment in *taz* mice. While all of the factors contributing to the improved exercise performance in *taz* mice are not known, increased mitochondrial biogenesis in spite of impaired respiration likely contributes. Mitochondria not

only proliferate in response to the increased metabolic demands of exercise, but within *taz* mice they appear to selectively remodel during proliferation, which perhaps limits the production of ROS.

Limitations

This study addressed only a narrow range of factors that contribute to enhanced exercise performance. Changes in biomechanics, substrate utilization, fiber type, and shifts in glycolytic metabolism either were not addressed or were not completely investigated. The use of an absolute exercise intensity rather than a relative one limits the comparisons that can be drawn between exercised animals. Additionally, the use of a ceilinged test limited the assessment of the efficacy of the exercise regimen within the WT mice. Furthermore, this study did not address the physical activity dimorphism in mice that is exhibited as higher physical activity in female mice over male mice. Utilizing other measures for mitochondrial content other than CS activity should also be done because CS activity may only indicate changes in the actual activity of CS and not the content of CS within mitochondria or SM.

There are numerous mitochondrial measures that were not measured, but the most relevant are the lack of a fat substrate and too few measures of mitochondrial antioxidant production. Due to the lack of a fat substrate the potential effect of UCP3 to influence leak was possibly masked. Multiple other ROS defense mechanisms, such as protein and activity levels of catalase, glutathione, glutathione peroxidase, glutathione reductase, and heat shock proteins exist beyond MnSOD protein content and were not examined and may serve to further explain the lower observed oxidative stress.

REFERENCES

1. Schlame, M. and M. Ren, *Barth syndrome, a human disorder of cardiolipin metabolism*. FEBS Lett, 2006. **580**(23): p. 5450-5.
2. Barth, P.G., et al., *An X-linked mitochondrial disease affecting cardiac muscle, skeletal muscle and neutrophil leucocytes*. J Neurol Sci, 1983. **62**(1-3): p. 327-55.
3. Barth, P.G., et al., *X-linked cardioskeletal myopathy and neutropenia (Barth syndrome) (MIM 302060)*. J Inherit Metab Dis, 1999. **22**(4): p. 555-67.
4. Schlame, M., et al., *The physical state of lipid substrates provides transacylation specificity for tafazzin*. Nat Chem Biol, 2012.
5. Bissler, J.J., et al., *Infantile dilated X-linked cardiomyopathy, G4.5 mutations, altered lipids, and ultrastructural malformations of mitochondria in heart, liver, and skeletal muscle*. Laboratory investigation; a journal of technical methods and pathology, 2002. **82**(3): p. 335-44.
6. Xu, Y., et al., *Characterization of lymphoblast mitochondria from patients with Barth syndrome*. Laboratory investigation; a journal of technical methods and pathology, 2005. **85**(6): p. 823-30.
7. Acehan, D., et al., *Cardiac and skeletal muscle defects in a mouse model of human Barth syndrome*. J Biol Chem, 2011. **286**(2): p. 899-908.
8. Soustek, M.S., et al., *Characterization of a transgenic short hairpin RNA-induced murine model of Tafazzin deficiency*. Hum Gene Ther, 2011. **22**(7): p. 865-71.
9. Phoon, C.K., et al., *Tafazzin knockdown in mice leads to a developmental cardiomyopathy with early diastolic dysfunction preceding myocardial noncompaction*. J Am Heart Assoc, 2012. **1**(2).
10. Cade, W.T., *Exercise Training in Barth Syndrome*. 2012.
11. Desai, K.H., et al., *Cardiovascular indexes in the mouse at rest and with exercise: new tools to study models of cardiac disease*. Am J Physiol, 1997. **272**(2 Pt 2): p. H1053-61.
12. Gleeson, T.T., W.J. Mullin, and K.M. Baldwin, *Cardiovascular responses to treadmill exercise in rats: effects of training*. J Appl Physiol, 1983. **54**(3): p. 789-93.
13. Allen, D.L., et al., *Cardiac and skeletal muscle adaptations to voluntary wheel running in the mouse*. J Appl Physiol, 2001. **90**(5): p. 1900-8.

14. Kemi, O.J., et al., *Intensity-controlled treadmill running in mice: cardiac and skeletal muscle hypertrophy*. J Appl Physiol, 2002. **93**(4): p. 1301-9.
15. Lumini-Oliveira, J., et al., *Endurance training reverts heart mitochondrial dysfunction, permeability transition and apoptotic signaling in long-term severe hyperglycemia*. Mitochondrion, 2011. **11**(1): p. 54-63.
16. Moraska, A., et al., *Treadmill running produces both positive and negative physiological adaptations in Sprague-Dawley rats*. Am J Physiol Regul Integr Comp Physiol, 2000. **279**(4): p. R1321-9.
17. Anversa, P., et al., *Morphometry of right ventricular hypertrophy induced by strenuous exercise in rat*. Am J Physiol, 1982. **243**(6): p. H856-61.
18. Anversa, P., et al., *Morphometry of exercise-induced right ventricular hypertrophy in the rat*. Circ Res, 1983. **52**(1): p. 57-64.
19. Kaplan, M.L., et al., *Cardiac adaptations to chronic exercise in mice*. Am J Physiol, 1994. **267**(3 Pt 2): p. H1167-73.
20. Wenz, T., et al., *Endurance exercise is protective for mice with mitochondrial myopathy*. J Appl Physiol, 2009. **106**(5): p. 1712-9.
21. Figueiredo, P.A., et al., *Impact of lifelong sedentary behavior on mitochondrial function of mice skeletal muscle*. J Gerontol A Biol Sci Med Sci, 2009. **64**(9): p. 927-39.
22. Schoepe, M., et al., *Exercise can induce temporary mitochondrial and contractile dysfunction linked to impaired respiratory chain complex activity*. Metabolism, 2012. **61**(1): p. 117-26.
23. Davies, K.J., et al., *Free radicals and tissue damage produced by exercise*. Biochem Biophys Res Commun, 1982. **107**(4): p. 1198-205.
24. Dubouchaud, H., et al., *Lactate transport activity in rat skeletal muscle sarcolemmal vesicles after acute exhaustive exercise*. J Appl Physiol, 1999. **87**(3): p. 955-61.
25. Hood, D.A., *Invited Review: contractile activity-induced mitochondrial biogenesis in skeletal muscle*. J Appl Physiol, 2001. **90**(3): p. 1137-57.
26. McArdle, A., et al., *Contractile activity-induced oxidative stress: cellular origin and adaptive responses*. Am J Physiol Cell Physiol, 2001. **280**(3): p. C621-7.
27. Irrcher, I., V. Ljubicic, and D.A. Hood, *Interactions between ROS and AMP kinase activity in the regulation of PGC-1alpha transcription in skeletal muscle cells*. Am J Physiol Cell Physiol, 2009. **296**(1): p. C116-23.

28. Strobel, N.A., et al., *Antioxidant supplementation reduces skeletal muscle mitochondrial biogenesis*. Med Sci Sports Exerc, 2011. **43**(6): p. 1017-24.
29. Pattwell, D.M., et al., *Release of reactive oxygen and nitrogen species from contracting skeletal muscle cells*. Free Radic Biol Med, 2004. **37**(7): p. 1064-72.
30. Holloszy, J.O., *Biochemical adaptations in muscle. Effects of exercise on mitochondrial oxygen uptake and respiratory enzyme activity in skeletal muscle*. J Biol Chem, 1967. **242**(9): p. 2278-82.
31. Jiang, N., et al., *Upregulation of uncoupling protein-3 in skeletal muscle during exercise: a potential antioxidant function*. Free Radic Biol Med, 2009. **46**(2): p. 138-45.
32. Ljubcic, V., P.J. Adhihetty, and D.A. Hood, *Role of UCP3 in state 4 respiration during contractile activity-induced mitochondrial biogenesis*. J Appl Physiol, 2004. **97**(3): p. 976-83.
33. Boss, O., et al., *Uncoupling protein-3 expression in rodent skeletal muscle is modulated by food intake but not by changes in environmental temperature*. J Biol Chem, 1998. **273**(1): p. 5-8.
34. Boss, O., et al., *Effect of endurance training on mRNA expression of uncoupling proteins 1, 2, and 3 in the rat*. FASEB J, 1998. **12**(3): p. 335-9.
35. Samec, S., J. Seydoux, and A.G. Dulloo, *Role of UCP homologues in skeletal muscles and brown adipose tissue: mediators of thermogenesis or regulators of lipids as fuel substrate?* FASEB J, 1998. **12**(9): p. 715-24.
36. Cadenas, S., et al., *UCP2 and UCP3 rise in starved rat skeletal muscle but mitochondrial proton conductance is unchanged*. FEBS Lett, 1999. **462**(3): p. 257-60.
37. Jones, T.E., et al., *Exercise induces an increase in muscle UCP3 as a component of the increase in mitochondrial biogenesis*. Am J Physiol Endocrinol Metab, 2003. **284**(1): p. E96-101.
38. Putman, C.T., et al., *Chronic low-frequency stimulation upregulates uncoupling protein-3 in transforming rat fast-twitch skeletal muscle*. Am J Physiol Regul Integr Comp Physiol, 2004. **287**(6): p. R1419-26.
39. Schrauwen, P. and M. Hesselink, *Uncoupling protein 3 and physical activity: the role of uncoupling protein 3 in energy metabolism revisited*. Proc Nutr Soc, 2003. **62**(3): p. 635-43.
40. Tsuboyama-Kasaoka, N., et al., *Up-regulation of uncoupling protein 3 (UCP3) mRNA by exercise training and down-regulation of UCP3 by denervation in skeletal muscles*. Biochem Biophys Res Commun, 1998. **247**(2): p. 498-503.

41. Divakaruni, A.S. and M.D. Brand, *The regulation and physiology of mitochondrial proton leak*. Physiology (Bethesda), 2011. **26**(3): p. 192-205.
42. Echtay, K.S., et al., *Uncoupling proteins 2 and 3 are highly active H(+) transporters and highly nucleotide sensitive when activated by coenzyme Q (ubiquinone)*. Proceedings of the National Academy of Sciences of the United States of America, 2001. **98**(4): p. 1416-21.
43. Zackova, M., et al., *Activating omega-6 polyunsaturated fatty acids and inhibitory purine nucleotides are high affinity Ligands for novel mitochondrial uncoupling proteins UCP2 and UCP3*. Journal of Biological Chemistry, 2003. **278**(23): p. 20761-20769.
44. Aguirre, E. and S. Cadenas, *GDP and carboxyatractylate inhibit 4-hydroxynonenal-activated proton conductance to differing degrees in mitochondria from skeletal muscle and heart*. Biochim Biophys Acta, 2010. **1797**(10): p. 1716-26.
45. Himms-Hagen, J. and M.E. Harper, *Physiological role of UCP3 may be export of fatty acids from mitochondria when fatty acid oxidation predominates: an hypothesis*. Exp Biol Med (Maywood), 2001. **226**(2): p. 78-84.
46. Schrauwen, P., J. Hoeks, and M.K. Hesselink, *Putative function and physiological relevance of the mitochondrial uncoupling protein-3: involvement in fatty acid metabolism?* Prog Lipid Res, 2006. **45**(1): p. 17-41.
47. Zhou, M., et al., *UCP-3 expression in skeletal muscle: effects of exercise, hypoxia, and AMP-activated protein kinase*. Am J Physiol Endocrinol Metab, 2000. **279**(3): p. E622-9.
48. Brand, M.D., et al., *Oxidative damage and phospholipid fatty acyl composition in skeletal muscle mitochondria from mice underexpressing or overexpressing uncoupling protein 3*. The Biochemical journal, 2002. **368**(Pt 2): p. 597-603.
49. Seifert, E.L., et al., *Essential role for uncoupling protein-3 in mitochondrial adaptation to fasting but not in fatty acid oxidation or fatty acid anion export*. J Biol Chem, 2008. **283**(37): p. 25124-31.
50. Brinkworth, R.I. and C.J. Masters, *The turnover of lactate dehydrogenase in skeletal muscle of the mouse. Influence of fibre type and exercise regimen*. Biochim Biophys Acta, 1978. **540**(1): p. 1-12.
51. Leger, L.A. and A.W. Taylor, *The chronic effects of continuous and intermittent running upon lactate dehydrogenase activity of heart, fast and slow twitch muscles in the rat*. J Physiol (Paris), 1982. **78**(6): p. 499-506.

52. Salminen, A., V. Vihko, and L. Pilstrom, *Effect of endurance training on the capacity of red and white skeletal muscle of mouse to oxidize carboxyl-14C-labelled palmitate*. Acta Physiol Scand, 1977. **101**(3): p. 318-28.
53. Ji, L.L., F.W. Stratman, and H.A. Lardy, *Chronic exercise training alters kinetic properties of rat skeletal muscle and myocardial lactate dehydrogenase*. FEBS Lett, 1986. **208**(2): p. 297-300.
54. E, L., et al., *Effect of Exercise on Mouse Liver and Brain Bioenergetic Infrastructures*. Exp Physiol, 2012.
55. Bonen, A. and K.J. McCullagh, *Effects of exercise on lactate transport into mouse skeletal muscles*. Can J Appl Physiol, 1994. **19**(3): p. 275-85.
56. Thomas, C., et al., *Effects of acute and chronic exercise on sarcolemmal MCT1 and MCT4 contents in human skeletal muscles: current status*. Am J Physiol Regul Integr Comp Physiol, 2012. **302**(1): p. R1-14.
57. Yoshida, Y., et al., *Relationship between skeletal muscle MCT1 and accumulated exercise during voluntary wheel running*. J Appl Physiol, 2004. **97**(2): p. 527-34.
58. Bonen, A., et al., *Short-term training increases human muscle MCT1 and femoral venous lactate in relation to muscle lactate*. Am J Physiol, 1998. **274**(1 Pt 1): p. E102-7.
59. Pilegaard, H., et al., *Effect of high-intensity exercise training on lactate/H⁺ transport capacity in human skeletal muscle*. Am J Physiol, 1999. **276**(2 Pt 1): p. E255-61.
60. Green, H., et al., *Increases in muscle MCT are associated with reductions in muscle lactate after a single exercise session in humans*. Am J Physiol Endocrinol Metab, 2002. **282**(1): p. E154-60.
61. Coles, L., et al., *Exercise rapidly increases expression of the monocarboxylate transporters MCT1 and MCT4 in rat muscle*. J Physiol, 2004. **561**(Pt 1): p. 253-61.
62. Bonen, A., et al., *Isoform-specific regulation of the lactate transporters MCT1 and MCT4 by contractile activity*. Am J Physiol Endocrinol Metab, 2000. **279**(5): p. E1131-8.
63. McCullagh, K.J., et al., *Role of the lactate transporter (MCT1) in skeletal muscles*. Am J Physiol, 1996. **271**(1 Pt 1): p. E143-50.
64. McCullagh, K.J., et al., *Chronic electrical stimulation increases MCT1 and lactate uptake in red and white skeletal muscle*. Am J Physiol, 1997. **273**(2 Pt 1): p. E239-46.
65. Bishop, D., et al., *High-intensity exercise acutely decreases the membrane content of MCT1 and MCT4 and buffer capacity in human skeletal muscle*. J Appl Physiol, 2007. **102**(2): p. 616-21.

66. Cosson, L., et al., *Barth syndrome in a female patient*. Mol Genet Metab, 2012. **106**(1): p. 115-20.
67. Chicco, A.J. and G.C. Sparagna, *Role of cardiolipin alterations in mitochondrial dysfunction and disease*. Am J Physiol Cell Physiol, 2007. **292**(1): p. C33-44.
68. Schlame, M., D. Rua, and M.L. Greenberg, *The biosynthesis and functional role of cardiolipin*. Progress in lipid research, 2000. **39**(3): p. 257-88.
69. Schlame, M. and B. Rustow, *Lysocardiolipin formation and reacylation in isolated rat liver mitochondria*. The Biochemical journal, 1990. **272**(3): p. 589-95.
70. Vendelin, M., et al., *Mitochondrial regular arrangement in muscle cells: a "crystal-like" pattern*. Am J Physiol Cell Physiol, 2005. **288**(3): p. C757-67.
71. Gu, Z., et al., *Aberrant cardiolipin metabolism in the yeast taz1 mutant: a model for Barth syndrome*. Mol Microbiol, 2004. **51**(1): p. 149-58.
72. Khuchua, Z., et al., *A zebrafish model of human Barth syndrome reveals the essential role of tafazzin in cardiac development and function*. Circ Res, 2006. **99**(2): p. 201-8.
73. Xu, Y., et al., *A Drosophila model of Barth syndrome*. Proceedings of the National Academy of Sciences of the United States of America, 2006. **103**(31): p. 11584-8.
74. Mole, P.A., L.B. Oscai, and J.O. Holloszy, *Adaptation of muscle to exercise. Increase in levels of palmityl Coa synthetase, carnitine palmityltransferase, and palmityl Coa dehydrogenase, and in the capacity to oxidize fatty acids*. J Clin Invest, 1971. **50**(11): p. 2323-30.
75. Hickson, R.C., *Skeletal muscle cytochrome c and myoglobin, endurance, and frequency of training*. J Appl Physiol, 1981. **51**(3): p. 746-9.
76. Harrison, B.C., et al., *Skeletal muscle adaptations in response to voluntary wheel running in myosin heavy chain null mice*. J Appl Physiol, 2002. **92**(1): p. 313-22.
77. Dudley, G.A., W.M. Abraham, and R.L. Terjung, *Influence of exercise intensity and duration on biochemical adaptations in skeletal muscle*. J Appl Physiol, 1982. **53**(4): p. 844-50.
78. Daussin, F.N., et al., *Different timing of changes in mitochondrial functions following endurance training*. Med Sci Sports Exerc, 2012. **44**(2): p. 217-24.
79. Baar, K., et al., *Adaptations of skeletal muscle to exercise: rapid increase in the transcriptional coactivator PGC-1*. FASEB J, 2002. **16**(14): p. 1879-86.

80. Barnard, R.J., V.R. Edgerton, and J.B. Peter, *Effect of exercise on skeletal muscle. I. Biochemical and histochemical properties*. J Appl Physiol, 1970. **28**(6): p. 762-6.
81. Judge, S., et al., *Exercise by lifelong voluntary wheel running reduces subsarcolemmal and interfibrillar mitochondrial hydrogen peroxide production in the heart*. Am J Physiol Regul Integr Comp Physiol, 2005. **289**(6): p. R1564-72.
82. Rolfe, D.F. and M.D. Brand, *Contribution of mitochondrial proton leak to skeletal muscle respiration and to standard metabolic rate*. Am J Physiol, 1996. **271**(4 Pt 1): p. C1380-9.
83. Rolfe, D.F. and M.D. Brand, *The physiological significance of mitochondrial proton leak in animal cells and tissues*. Bioscience reports, 1997. **17**(1): p. 9-16.
84. Affourtit, C. and M.D. Brand, *Stronger control of ATP/ADP by proton leak in pancreatic beta-cells than skeletal muscle mitochondria*. The Biochemical journal, 2006. **393**(Pt 1): p. 151-9.
85. Azzu, V., et al., *The regulation and turnover of mitochondrial uncoupling proteins*. Biochim Biophys Acta, 2010. **1797**(6-7): p. 785-91.
86. Brand, M.D., et al., *The basal proton conductance of mitochondria depends on adenine nucleotide translocase content*. The Biochemical journal, 2005. **392**(Pt 2): p. 353-62.
87. Brand, M.D., et al., *Proton conductance and fatty acyl composition of liver mitochondria correlates with body mass in birds*. The Biochemical journal, 2003. **376**(Pt 3): p. 741-8.
88. Fontaine, E.M., et al., *Effect of polyunsaturated fatty acids deficiency on oxidative phosphorylation in rat liver mitochondria*. Biochim Biophys Acta, 1996. **1276**(3): p. 181-7.
89. Porter, R.K., A.J. Hulbert, and M.D. Brand, *Allometry of mitochondrial proton leak: influence of membrane surface area and fatty acid composition*. Am J Physiol, 1996. **271**(6 Pt 2): p. R1550-60.
90. Brookes, P.S., A.J. Hulbert, and M.D. Brand, *The proton permeability of liposomes made from mitochondrial inner membrane phospholipids: no effect of fatty acid composition*. Biochim Biophys Acta, 1997. **1330**(2): p. 157-64.
91. Cadenas, S., et al., *The basal proton conductance of skeletal muscle mitochondria from transgenic mice overexpressing or lacking uncoupling protein-3*. J Biol Chem, 2002. **277**(4): p. 2773-8.
92. Marcinek, D.J., et al., *Reduced mitochondrial coupling in vivo alters cellular energetics in aged mouse skeletal muscle*. J Physiol, 2005. **569**(Pt 2): p. 467-73.

93. Nicholls, D.G., *A history of UCPI*. Biochem Soc Trans, 2001. **29**(Pt 6): p. 751-5.
94. Cannon, B. and J. Nedergaard, *Brown adipose tissue: function and physiological significance*. Physiol Rev, 2004. **84**(1): p. 277-359.
95. Azzu, V. and M.D. Brand, *The on-off switches of the mitochondrial uncoupling proteins*. Trends Biochem Sci, 2010. **35**(5): p. 298-307.
96. Azzu, V., S.A. Mookerjee, and M.D. Brand, *Rapid turnover of mitochondrial uncoupling protein 3*. Biochem J, 2010. **426**(1): p. 13-7.
97. Goglia, F. and V.P. Skulachev, *A function for novel uncoupling proteins: antioxidant defense of mitochondrial matrix by translocating fatty acid peroxides from the inner to the outer membrane leaflet*. FASEB J, 2003. **17**(12): p. 1585-91.
98. Solanes, G., et al., *The human uncoupling protein-3 gene promoter requires MyoD and is induced by retinoic acid in muscle cells*. FASEB J, 2000. **14**(14): p. 2141-3.
99. Amat, R., et al., *SIRT1 is involved in glucocorticoid-mediated control of uncoupling protein-3 gene transcription*. J Biol Chem, 2007. **282**(47): p. 34066-76.
100. Boss, O., et al., *Uncoupling protein-3: a new member of the mitochondrial carrier family with tissue-specific expression*. FEBS Lett, 1997. **408**(1): p. 39-42.
101. Vidal-Puig, A., et al., *UCP3: an uncoupling protein homologue expressed preferentially and abundantly in skeletal muscle and brown adipose tissue*. Biochem Biophys Res Commun, 1997. **235**(1): p. 79-82.
102. Papa, S. and V.P. Skulachev, *Reactive oxygen species, mitochondria, apoptosis and aging*. Mol Cell Biochem, 1997. **174**(1-2): p. 305-19.
103. Crescenzo, R., et al., *Skeletal muscle mitochondrial oxidative capacity and uncoupling protein 3 are differently influenced by semistarvation and refeeding*. FEBS Lett, 2003. **544**(1-3): p. 138-42.
104. Schrauwen, P., et al., *Effect of acute exercise on uncoupling protein 3 is a fat metabolism-mediated effect*. Am J Physiol Endocrinol Metab, 2002. **282**(1): p. E11-7.
105. Bezaire, V., et al., *Constitutive UCP3 overexpression at physiological levels increases mouse skeletal muscle capacity for fatty acid transport and oxidation*. FASEB J, 2005. **19**(8): p. 977-9.
106. Bezaire, V., et al., *Effects of fasting on muscle mitochondrial energetics and fatty acid metabolism in Ucp3(-/-) and wild-type mice*. Am J Physiol Endocrinol Metab, 2001. **281**(5): p. E975-82.

107. Cortright, R.N., et al., *Regulation of skeletal muscle UCP-2 and UCP-3 gene expression by exercise and denervation*. Am J Physiol, 1999. **276**(1 Pt 1): p. E217-21.
108. Hildebrandt, A.L., H. Pilegaard, and P.D. Neufer, *Differential transcriptional activation of select metabolic genes in response to variations in exercise intensity and duration*. Am J Physiol Endocrinol Metab, 2003. **285**(5): p. E1021-7.
109. Anderson, E.J., H. Yamazaki, and P.D. Neufer, *Induction of endogenous uncoupling protein 3 suppresses mitochondrial oxidant emission during fatty acid-supported respiration*. J Biol Chem, 2007. **282**(43): p. 31257-66.
110. Vidal-Puig, A.J., et al., *Energy metabolism in uncoupling protein 3 gene knockout mice*. J Biol Chem, 2000. **275**(21): p. 16258-66.
111. Fernstrom, M., M. Tonkonogi, and K. Sahlin, *Effects of acute and chronic endurance exercise on mitochondrial uncoupling in human skeletal muscle*. J Physiol, 2004. **554**(Pt 3): p. 755-63.
112. Russell, A.P., et al., *UCP3 protein regulation in human skeletal muscle fibre types I, IIa and IIx is dependent on exercise intensity*. J Physiol, 2003. **550**(Pt 3): p. 855-61.
113. Russell, A.P., et al., *UCP3 protein expression is lower in type I, IIa and IIx muscle fiber types of endurance-trained compared to untrained subjects*. Pflugers Arch, 2003. **445**(5): p. 563-9.
114. Bonen, A., M. Heynen, and H. Hatta, *Distribution of monocarboxylate transporters MCT1-MCT8 in rat tissues and human skeletal muscle*. Appl Physiol Nutr Metab, 2006. **31**(1): p. 31-9.
115. Bonen, A., et al., *Abundance and subcellular distribution of MCT1 and MCT4 in heart and fast-twitch skeletal muscles*. Am J Physiol Endocrinol Metab, 2000. **278**(6): p. E1067-77.
116. Benton, C.R., et al., *Monocarboxylate transporters in subsarcolemmal and intermyofibrillar mitochondria*. Biochem Biophys Res Commun, 2004. **323**(1): p. 249-53.
117. Johannsson, E., et al., *Cellular and subcellular expression of the monocarboxylate transporter MCT1 in rat heart. A high-resolution immunogold analysis*. Circ Res, 1997. **80**(3): p. 400-7.
118. Yoshida, Y., et al., *Negligible direct lactate oxidation in subsarcolemmal and intermyofibrillar mitochondria obtained from red and white rat skeletal muscle*. J Physiol, 2007. **582**(Pt 3): p. 1317-35.

119. Thomas, C., et al., *Monocarboxylate transporters, blood lactate removal after supramaximal exercise, and fatigue indexes in humans*. J Appl Physiol, 2005. **98**(3): p. 804-9.
120. Bishop, D., et al., *Effects of high-intensity training on muscle lactate transporters and postexercise recovery of muscle lactate and hydrogen ions in women*. Am J Physiol Regul Integr Comp Physiol, 2008. **295**(6): p. R1991-8.
121. Lin, R.Y., et al., *Human monocarboxylate transporter 2 (MCT2) is a high affinity pyruvate transporter*. J Biol Chem, 1998. **273**(44): p. 28959-65.
122. Gladden, L.B., *Is there an intracellular lactate shuttle in skeletal muscle?* J Physiol, 2007. **582**(Pt 3): p. 899.
123. Brooks, G.A. and T. Hashimoto, *Investigation of the lactate shuttle in skeletal muscle mitochondria*. J Physiol, 2007. **584**(Pt 2): p. 705-6;author reply 707-8.
124. Gladden, L.B., *A lactatic perspective on metabolism*. Med Sci Sports Exerc, 2008. **40**(3): p. 477-85.
125. Cruz, R.S., et al., *Intracellular shuttle: the lactate aerobic metabolism*. ScientificWorldJournal, 2012. **2012**: p. 420984.
126. Kline, E.S., et al., *Localization of L-lactate dehydrogenase in mitochondria*. Arch Biochem Biophys, 1986. **246**(2): p. 673-80.
127. Brandt, R.B., et al., *Lactate dehydrogenase in rat mitochondria*. Arch Biochem Biophys, 1987. **259**(2): p. 412-22.
128. Rasmussen, H.N., G. van Hall, and U.F. Rasmussen, *Lactate dehydrogenase is not a mitochondrial enzyme in human and mouse vastus lateralis muscle*. J Physiol, 2002. **541**(Pt 2): p. 575-80.
129. Sahlin, K., et al., *No evidence of an intracellular lactate shuttle in rat skeletal muscle*. J Physiol, 2002. **541**(Pt 2): p. 569-74.
130. Brooks, G.A., et al., *Role of mitochondrial lactate dehydrogenase and lactate oxidation in the intracellular lactate shuttle*. Proc Natl Acad Sci U S A, 1999. **96**(3): p. 1129-34.
131. Desai, K.H., et al., *Phospholamban deficiency does not compromise exercise capacity*. Am J Physiol, 1999. **276**(4 Pt 2): p. H1172-7.
132. Hoffman-Goetz, L., et al., *Exercise stress alters murine lymphocyte subset distribution in spleen, lymph nodes and thymus*. Clin Exp Immunol, 1989. **76**(2): p. 307-10.

133. Fernando, P., A. Bonen, and L. Hoffman-Goetz, *Predicting submaximal oxygen consumption during treadmill running in mice*. Can J Physiol Pharmacol, 1993. **71**(10-11): p. 854-7.
134. Schefer, V. and M.I. Talan, *Oxygen consumption in adult and AGED C57BL/6J mice during acute treadmill exercise of different intensity*. Exp Gerontol, 1996. **31**(3): p. 387-92.
135. Billat, V.L., et al., *Inter- and intrastain variation in mouse critical running speed*. J Appl Physiol, 2005. **98**(4): p. 1258-63.
136. Sparagna, G.C., et al., *Loss of cardiac tetralinoleoyl cardiolipin in human and experimental heart failure*. J Lipid Res, 2007. **48**(7): p. 1559-70.
137. Gershoni, J.M. and G.E. Palade, *Electrophoretic transfer of proteins from sodium dodecyl sulfate-polyacrylamide gels to a positively charged membrane filter*. Anal Biochem, 1982. **124**(2): p. 396-405.
138. Ferreira, J.C., et al., *Maximal lactate steady state in running mice: effect of exercise training*. Clin Exp Pharmacol Physiol, 2007. **34**(8): p. 760-5.
139. Macambira, S.G., et al., *Granulocyte colony-stimulating factor treatment in chronic Chagas disease: preservation and improvement of cardiac structure and function*. FASEB J, 2009. **23**(11): p. 3843-50.
140. Jiao, Q., et al., *Sarcalumenin is essential for maintaining cardiac function during endurance exercise training*. Am J Physiol Heart Circ Physiol, 2009. **297**(2): p. H576-82.
141. Chen, Q., et al., *Production of reactive oxygen species by mitochondria: central role of complex III*. J Biol Chem, 2003. **278**(38): p. 36027-31.

APPENDIX I

MODIFIED SKELETAL MUSCLE MITOCHONDRIAL ISOLATION PROCEDURE

Skeletal Muscle Mitochondria Isolation Procedure:

During isolation keep everything on ice

1. Remove whole hind limb and tibialis anterior
 - a. Put muscle in CP0 ~5 ml/container
2. Weigh muscle
3. Remove connective tissue and weigh then place back in CP0
4. Mince tissues with pairs of scissors in CP0.
5. Transfer to 15 ml conicals and “wash” spin at lowest G, discard supernatant.
6. Bring the pellet to ~4 ml with CP0
7. Add 1ml with (10 mg trypsin/g tissue) (dilute trypsin to 1:1 with washed tissue not volume) trypsin, bring to 5 ml
8. Agitate/rock in trypsin with occasional vortex for 8 minutes (no more than 10)
9. Run at least 5 drill plunges (~7) with Teflon homogenizer in homogenizing tubes
10. Add 1 ml CP2 (ideally want 1:1 tissue with trypsin to CP2) to stop trypsin
11. Transfer homogenate to 2 ml centrifuge tubes below 1 ml
12. Centrifuge at 11500 G for 10 min (separates pellet from Trypsin) and discard the supernatant
13. Resuspend with 1 ml CP2
14. Spin at 1400 G for 10 min.
 - a. Non-mitochondria pelleted. Want supernatant. Be careful to avoid cloudy middle layer
15. While transfer pipetting the supernatant, gently “shoot” the supernatant through cheesecloth into new centrifuge tubes

16. Resuspend pellet with < 1 ml CP2
17. Spin at 1400 G for 10 min and pull off any remaining supernatant and transfer through cheesecloth
18. Spin supernatant tubes at 6700 G for 20 min.
19. Discard supernatant (pellet is mito)
20. Resuspend w/ CP2 (only enough to combine same sample tubes)
21. Spin at 6700 G for 10 min
22. Pour off supernatant and resuspend with ~1 ml KME
23. Spin at 6700 G for 10 min and pour off supernatant
24. "Dry" and tap out remaining liquid.
25. Add ~250 μ l KME resuspend (vortex fully) this suspension is isolated mitochondria.

APPENDIX II

PERMEABILIZED FIBERS

Permeabilized Fibers

Procedure

After animals were terminally anesthetized with 100mpk of sodium pentobarbital, animals were weighed and then euthanized by midline thoracotomy and removal of the heart. Upon removal, hearts were cleaned of fatty tissue, drained of blood, weighed, and frozen in liquid nitrogen. After euthanasia, left and right gastrocnemius (gastroc) and soleus (sol) muscles were dissected away and weighed. After weighing, sol were placed in ice-cold BIOPS solution. Sol were teased apart in BIOPS for approximately 7 min. The objective of the teasing was to separate individual fibers as much as possible without causing damage to the fibers. After teasing, fibers were placed in Saponin for 30 minutes (in future studies this time was reduced to 20 minutes) and rocked. Fibers were rocked for 30 min in MIR06 after Saponin treatment (in future studies fibers were washed in separated MIR06 baths for 10 min apiece). After washing, fibers were weighed and immediately placed in the calibrated two-channel high resolution respirometer with MIR06 in the respiration chambers. Substrate titrations were then administered at the same concentrations as used with isolated mitochondria. Oxygen saturation was maintained using titrations of H_2O_2 , which was converted to O_2 by the catalase in the MIR06.

Results

Malate-pyruvate oxidation was slightly depressed in *taz* mice compared to WT mice (18.68 vs. 16.44, WTS vs. TazS). Malate-lactate oxidation was slightly elevated in *taz* mice (6.26 vs. 6.36, WTS vs. TazS) (figure 1)

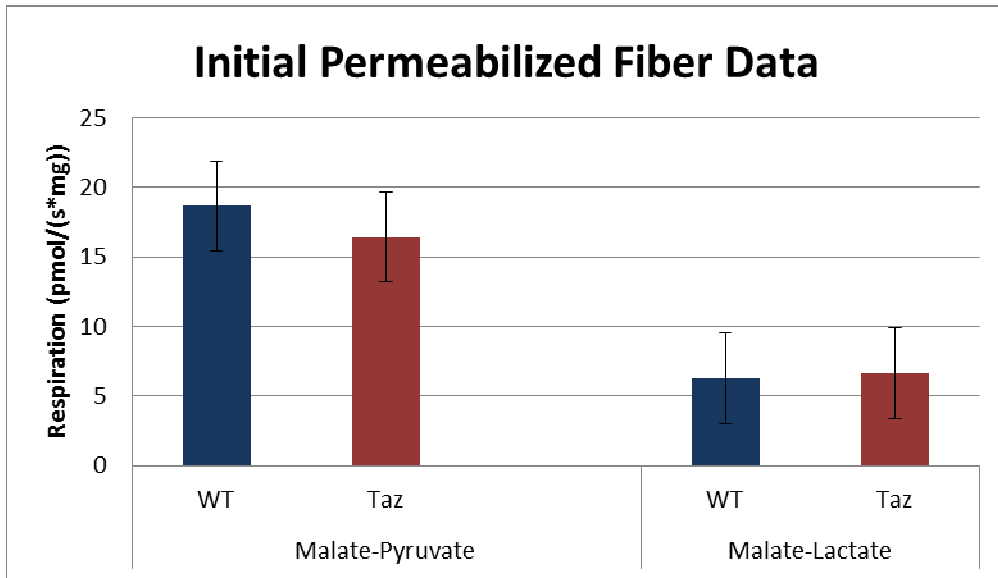


Figure 11. Means of permeabilized fiber oxidation with MP and ML. Error bars are \pm SEM.

Discussion

Permeabilized fiber data were inconsistent and did not produce a clean signal. After 17 runs of the O2k, fiber data were not approximating isolated mitochondria data, so the decision was made to use a practiced method. The investigator has gained more experience successfully utilizing the permeabilized fiber technique. It appears that the high amounts of connective tissue that accompany the sol makes it more difficult to tease than a biopsy taken from a well-developed muscle belly. In addition, the altered permeabilizing and washing procedures seemed to produce a slightly cleaner signal when the technique was tried again in sol for another project.